Flexible Wearable Electronics: Present State and Future Development

Qi Zhang[1], Jianjia Mu[2], Xiao Liu[3], Xuanwen Gao[2], Zhaomeng Liu[2], and Wen-Bin Luo[2]

[1]Taiyuan University of Technology College of Mechanical and Vehicle Engineering
[2]Northeastern University
[3]Taiyuan University of Technology

March 29, 2023

Abstract

Wearable electronics are expected to be light, durable, flexible, and comfortable. Many fibrous, planar and tridimensional structures have been designed to realize flexible devices that can sustain geometrical deformations, such as bending, twisting, folding, and stretching normally at ambient conditions. As a flexible electrode for batteries or other devices, it possess favorable mechanical strength and large specific capacity and preserve efficient ionic and electronic conductivity with a certain shape, structure and function. To fulfill flexible energy-storage devices, much effort has been devoted to design of structures and materials with mechanical characteristics. This review attempts to critically review the state-of-arts with respect to materials, and structural design of devices as well as applications of the wearable electronic products. Finally, discussion present regarding to limitations of current materials, fabrication techniques, devices concerning manufacturability and performance as well as scientific understanding that must be improved prior to their wide adoption.

Introduction

Due to the tension of living under high pressure, light, portable, functional goods have been more and more important to make our life easier. Portable electronics such as wireless sensors, roll-up displays, electronic skins, flexible smartphones are light in weight and come into smaller sizes which can easily be carried around. New generation flexible electronic devices require a flexible and reliable power sources with high energy density, long cycle life, excellent rate capability and a compatible electrolytes and separators. Besides, safety and cost should also be considered in the practical application.[1-4] And the flexible and lightweight energy storage system is robust under geometry deformation without compromising their performance.

As usual, the mechanical reliability of flexible energy storage devices include electrical performance retention and deformation endurance. As a flexible electrode, it should possess favorable mechanical strength and large specific capacity. And the electrodes need to preserve efficient ionic and electronic conductivity during cycling. Much effort has been conducted toward the design of structures and materials with mechanical characteristics to realize flexible devices that can sustain geometrical deformations, such as bending, twisting, folding, and stretching (**Figure 1**).[5, 6] In contrast with the conventional electrodes, the flexible electrodes are usually fabricated without binder, conductive additive, or even current collector. Inspired by this, flexible energy storage systems such as flexible alkaline batteries, [7] flexible zinc carbon batteries[8] all-polymer batteries,[9] flexible rechargeable ion batteries[10, 11] and flexible supercapacitors (SCs)[12] have been explored and investigated. Among these, flexible rechargeable batteries (e.g., lithium ion batteries, sodium ion batteries, Lithium-sulfur, *etc* .) are very promising.[13, 14] They have exhibited performance limitations in

their short cycle life, relatively slow charging–discharging rates and lower power densities. To compensate for the lower power densities of these batteries, supercapacitors, also known as electrochemical capacitors (ECs) or ultracapacitors, have emerged as considerable alternative candidates to batteries and offer a number of potential advantages in performance, including superior operating lifetimes, ultrafast charging-discharging rates, and high-power densities.[15-17] However, current electrodes with good electrochemical performance employed in batteries and supercapacitors are mainly based on relatively rigid and fragile electrodes and are unsuitable for flexible device fabrication because they show poor sustainability under complex stress environments. Meanwhile, the electrochemically inactive binder also could cause the loss of capacity and other safety problems.[18-20] Thus, the binder free electrodes for flexible energy storage devices emerged.

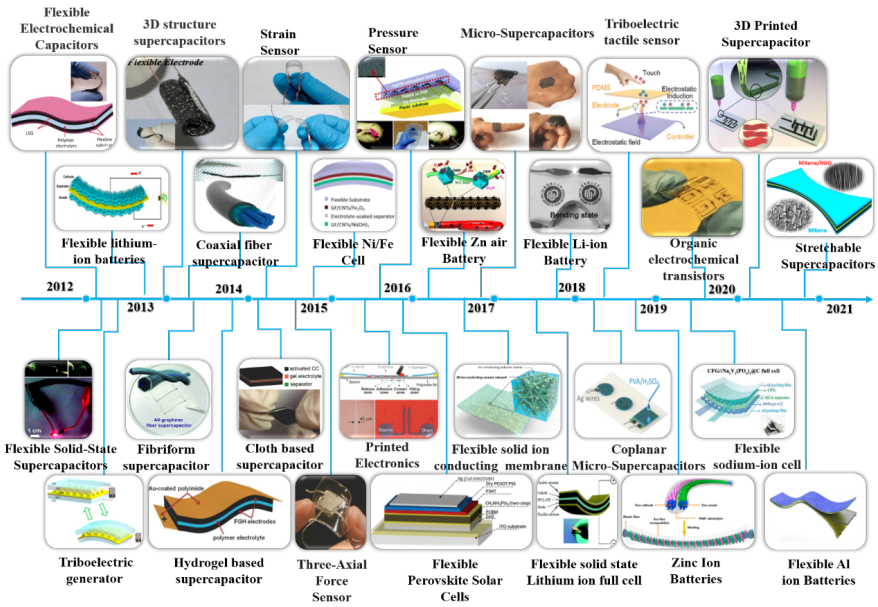

Figure 1 . The evolution of waist watches and mobile phones in our daily life. [21-47]

Based on recent development, there are two strategies for fabricating flexible electrodes or components: First, synthesizing flexible freestanding films of active materials; Second, depositing rigid active materials on flexible conductive or non-conducting substrates, a strong interaction between the active material and the substrate is generally required to maintain the structural integrity during deformation. We endow flexible and stretchable materials with favorable electrochemical performance or rigid high-performance material with flexible nature though engineering. A schematic sketch of flexible batteries, SCs and sensor with different designs and structures along with the types of electrode used in their fabrication is given in **Figure2** . This review concentrated on the recent progress on flexible energy-storage devices, including flexible batteries and supercapacitors (SCs) and sensors. In the first part, we review the latest fiber, planar and 3D based flexible devices with different solid-state electrolytes, and novel structures, along with their technological innovations and challenges. In the following section, a specific overview of the recent achievement about flexible electrolyte based on polymer, ceramic and polymer/ceramic electrolyte are given, combined with discussion of the problem and opportunities for the fabrication of the state-of-the-art flexible electrolyte. In the end, prospects and outlook on the future of flexible batteries are presented and discussed.

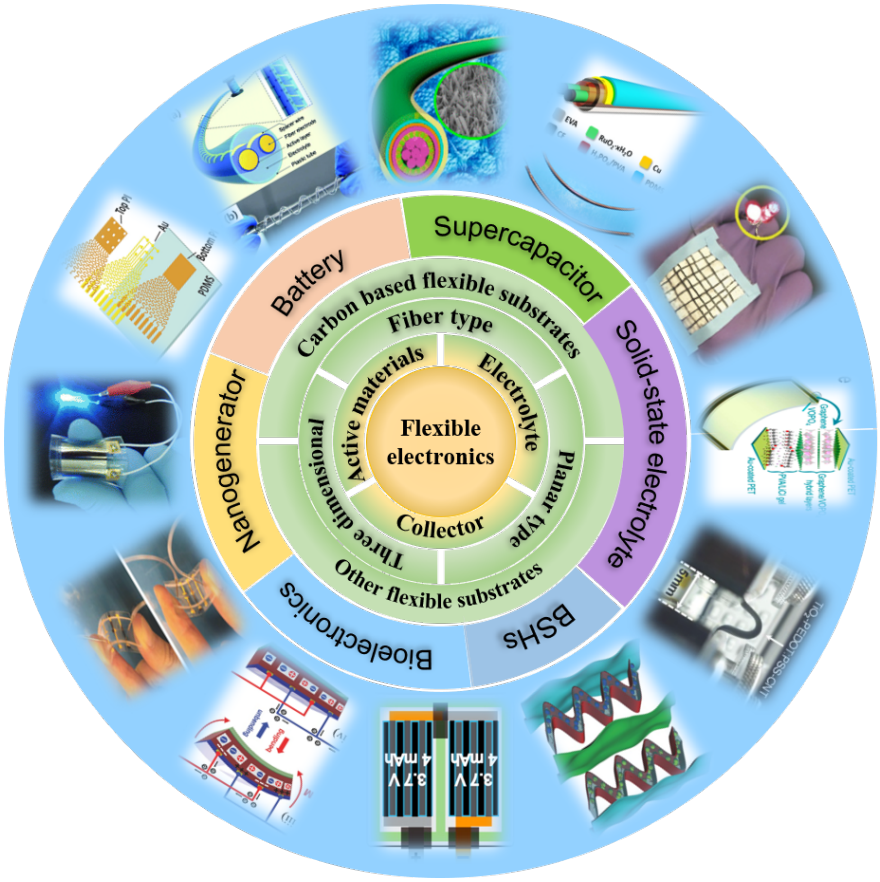

Figure 2 . Flexible energy storage devices and the types of electrode used in their fabrication.

2. Fiber-based wearable electronics

Typically, the fiber usually has a large aspect ratio with a thickness or diameter in the scale of micron meters. These fibers can be further converted into various shapes (*e.g.* yarns, fabrics, spacer fabrics *etc* .) through well established and cost-effective textile production processes. Meanwhile, the advanced nanoscience and nanotechnology has made it feasible to build electronic modules under a fiber technology and accelerate the miniaturization trend of electronic devices. Modern wearable electronics with the nature of fiber assemblies are endowed the advantage of textiles technologies, electrical engineering and electronics, and the superior capacity. The hierarchical nature of these fibrous structures (fiber - yarn - fabric, *etc* .) makes it particularly suitable for the fabrication of wearable electronics. This section reviews the current state of the fiber-based wearable electronics in the areas of energy conversion, healthcare, environmental monitoring, displays, human-machine interactivity and communication with the respect of conductive materials, fabrication techniques, electronic components, devices and applications of fiber-based wearable electronics.

2.1 Carbon nanotube based flexible electronics

To meet the gradually increasing demands of portable electronics, it is significant to develop a lightweight, flexible, and conformable electrodes for flexible electronics. For the realization of the fiber-based wearable electronics, the most important consideration is the development of sustainable flexible systems which support

high carrier mobility and good overall electrical performance, together with mechanical and environmental stability. Textile technologies offer tremendous opportunities to make sensors and other devices, built-in or embedded into the fabric-based network. So far, many composites such as reduced graphene oxide/nylon yarn, [48]Ag-silicone fibers, [49] fibers containing liquid metal alloy,[50]a conductive composite mat of silver nanoparticles and rubber fibers, and twisted graphene yarns[51] are designed for functional textiles, flexible and wearable battery devices. Among them, carbon-based materials are popular substrates for flexible electrode as they can act as both current collector and active materials.[52] For its favorable weavability, flexibility and conductivity, carbon-nanotube (CNT) fibers as a typical 1D conductive material has been widely used in the fabrication of flexible electrode, which can be woven to form wearable cloths.[40, 53] In **Figure** 3a, the $Li_4Ti_5O_{12}$ (LTO) and Li_2MnO_4 (LMO) particles were incorporated into two multi-walled carbon nanotube (MWCNT) threads by a soaking method, paired as anode and cathode to create a lithium-ion battery with a reversible capacity of 2.2 mAh m^{-1}. The elastic wire-shaped lithium-ion battery (**Figure** 3b) was assembled by winding above electrodes around an elastic substrate with a spring structure. When the battery was stretched by 100%, the illumination intensity of the LED has no obvious change.[54] Additionally, other functional guests (TiO_2, Si_3N_4, MnO_2, Si nanowires) had been incorporated into the wires to improve the specific capacity of the devices.[55-59] The composite electrodes are expected to combine their individual advantage of high specific capacity, flexibility and excellent conductivity. Peng *et al* . reported that a nanoscale Si layer was coated on the surface of the carbon nanotube sheets by atomic layer deposition (ALD). The core-shell structured CNT@Si composites are endowed the high specific capacitance of silicon and the good electrical conductivity of CNT (**Figure 3e**). Flexible composite fiber was obtained by a twisting treatment, which could bend for over a hundred cycles without an obvious decrease in the structure integrity. The specific capacity of it was maintained at 1460 mAh g^{-1} (96% of the initial specific capacity) after 100 times bending [**Figure 3(f-g**)]. The good electrochemical performance can be attribute to the core-sheath structure which could effectively counterbalance the volume change of Si. And the aligned CNT enhance the charge transport between the CNT and the Si. [55]

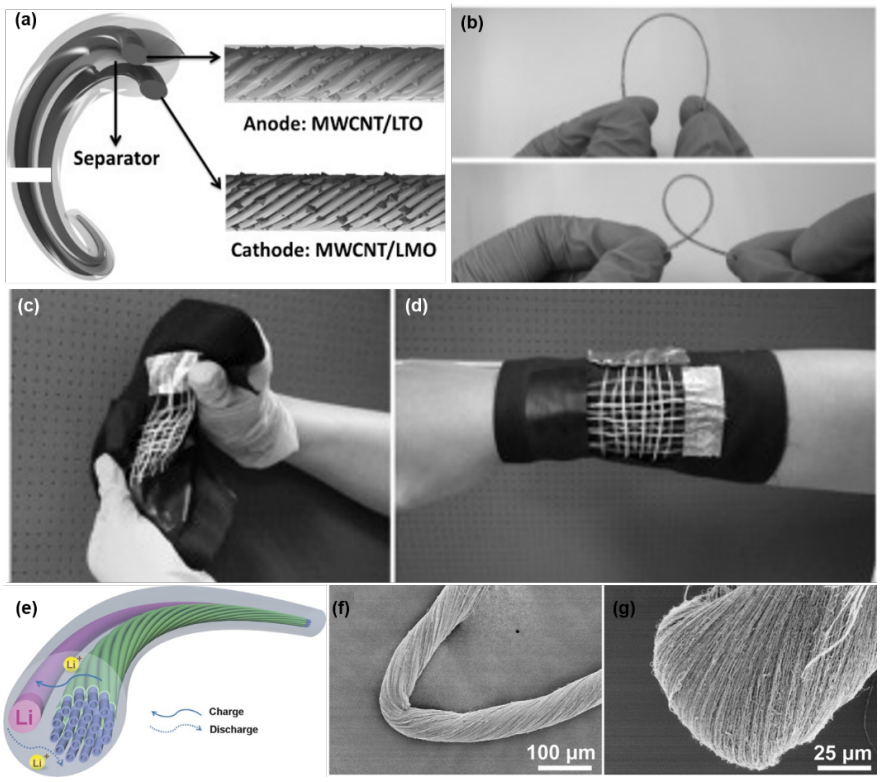

Figure 3. a) The aligned MWCNT/LTO and MWCNT/LMO composite yarns are paired as the anode and cathode, respectively. b) Photographs of a wire-shaped battery being deformed into different shapes. c, d) Wire-shaped batteries woven into flexible textiles. [54] e) illustration of a half lithium-ion battery based on the aligned MWCNT/Si composite fiber. f, g) SEM images of a bent aligned MWCNT/Si composite fiber.[55]

2.2 Graphene based flexible electronics

Besides, graphene fiber with high strength and electrical conductivity represents another ideal type of fiber electrode.[60, 61] It possesses the mechanical flexibility of common textile fibers and modified easily in comparison with the conventional carbon fibers.[62, 63] In 2012, Qu *et al* . fabricated the neat graphene fiber by a facile one-step dimensional-confined hydrothermal strategy. It has a tensile strength of 180 MPa and can be shaped to random geometry. The pliability of this fiber facilitates the weaving into various macroscopic objects.[64] Therefore, it has a great potential to apply in stimulus-responsive and electronic-textiles (**Figure** . 4a-4d). Along with the booming research on flexible batteries, motors, actuators, dye-sensitized photovoltaic wires, supercapacitors also have been designed based on the graphene fiber to expand its application.[42, 65-67] Gao *et al.* prepared continuous graphene-Ag fiber with high electrical conductivity (9.3×10^4 S m^{-1}) and current capacity (7.1×10^3 A cm^{-2}), rendering the composite fibers good stretchable conductors to be applied in soft circuits.[68] Compared with batteries, supercapacitors have a superior charge/discharge rate, ultrahigh power delivery, excellent cycle life and efficiency, a wide range of operating temperatures, and improved safety. Because of it is easily incorporated into textiles, the fiber-shaped supercapacitor attracted widespread interest. [69-71] Peng's group also reported much work about fiber-shaped devices based on the graphene.[54, 55, 57, 59] With the graphene fiber as the core, nanorod like polyaniline was deposited by an in-*situ*chemical polymerization strategy (**Figure** 4e). The fabricated core-sheath fibers were twisted into all solid-state yarn shaped supercapacitor with H_2SO_4/PVA gel electrolyte. The performance of this fiber type device under bending has no change (**Figure** 4f). Moreover, three red LEDs were lighted by four supercapacitors in series. [72] Wang *et al* prepared stretchable and self-healable supercapacitor by wrapping two parallel reduced graphene oxide fiber springs with a self-healing polymer shell (**Figure** 4g and 4h). At the power density of 7.32 mW cm^{-3}, a high energy of 0.94 mWh cm^{-3} was obtained. The capacitance retention is 82.4% after a large stretch (100%), while it is 54.2% after the third healing. It provides an essential strategy in next generation multifunctional electronic device. [73]

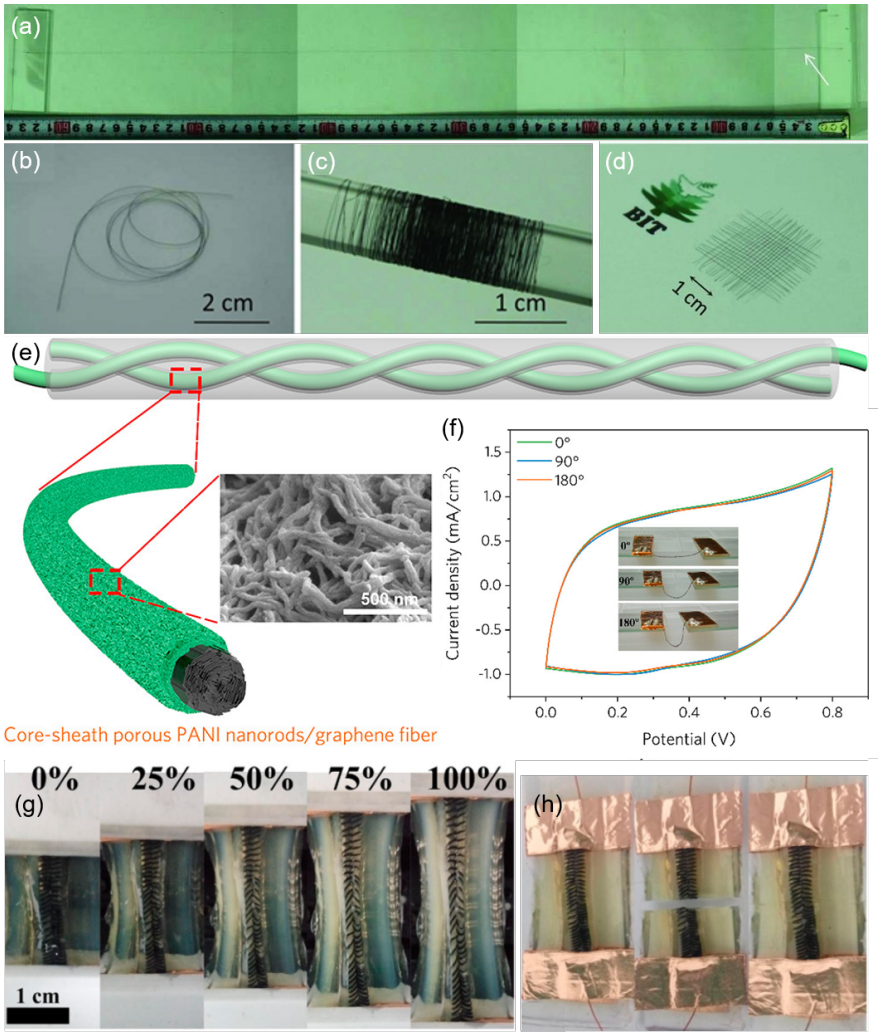

Figure 4. Morphology and flexibility of graphene fiber. Photograph of a single dry graphene fiber a) with a diameter of 33 μm and a length of 63 cm. b) a wet graphene fiber coiled individually in water. c) A dry graphene fiber coiled in bundle around the glass rod. d) The hand-knitted textile of graphene fibers.[64]e) Schematic diagram of the yarn-shaped supercapacitors. f) CV curves of all-solid-state GF@PANI FSSC bended with 0°, 90°, and 180°.[72] g) Photographs of the supercapacitor before and after stretching to 100%. h) Photographs of the supercapacitor before and after self-healing.[73]

2.3 Flexible electronics based on other substrates

Apart from the graphene and CNT, the conductive substrate like nickel fiber was also used to fabricated fiber-shaped devices. As depicted in**Figure 5a** , multiwalled carbon nanotubes and vanadium oxide were used as the coating layer of the current collector of Au wire to enhance the overall supercapacitor performance via pseudocapacitance. Each electrode was dipped into the PC–ACN–$LiClO_4$–PMMA electrolyte. [74] Then, two electrodes were twisted to form a wire-shaped supercapacitor (WSS). It delivered an area capacitance of 5.23 mF cm^{-2} at 0.2 mA cm^{-2}, the capacitance retention under shape deformation varied from 97 to 104%, reasonably constant and equivalent to the original capacitance. The nickel fiber with $Ni(OH)_2$-nanowire and the ordered mesoporous carbon fiber were twisted together with the KOH-PVA as the gel electrolyte, a flexible micro-supercapacitor was obtained after further vaporizing water from the gel electrolyte. It

presented 35.67 mF cm^{-2} and the charge/discharge performance of the fiber-shaped supercapacitor is almost independent of the bending states.[75] Wang *et al* . demonstrated that polyester yarns coated with Ni were utilized as current collectors for electrodes in all-solid- state yarn supercapacitors, as schemed in**Figure 3d** . The rGO layer was coated on the electrode as active materials. Two rGO-Ni-yarns in parallel, and poly(vinyl alcohol) (PVA)/H_3PO_4 gel as solid electrolyte and separator were assembled into a symmetric yarn supercapacitor.[76] After bending 1000 cycles by a motor, the capacitance of this yarn supercapacitor shows no significant difference. As for wearable energy-storing textiles, it can withstand harsh deformation. Five yarn supercapacitors were connected in series and were woven into a piece of fabric together with common cotton yarns. This soft energy-storing fabric can light a red light-emitting diode. In addition, flexible zinc ion batteries and other alkaline batteries have been fabricated. Huang *et al* . reported that bimetallic hydroxides could deliver higher capacity because of the synergistic effects between transition metal ions (**Figure 5b**). Zinc and nickel cobalt hydroxide nanosheets were electrodeposited on the highly conductive yarn. The solid-state yarn battery delivered maximum volumetric density of 8 mWh cm^{-3}. The device has shown good weavability, flexibility. [77] Zhi *et al* . also reported a flexible, high performance yarn Zinc ion battery using double-helix yarn electrodes and a cross-linked polyacrylamide (PAM) electrolyte.[27]

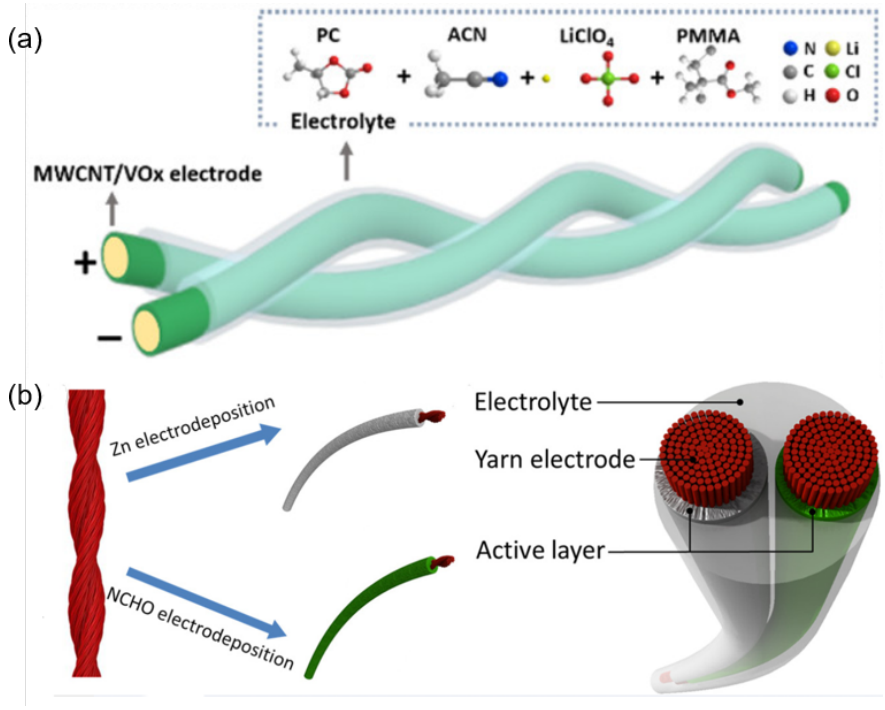

Figure 5. (a) The WSS with a 100 μm thick Au wire, coated with multiwalled carbon nanotubes (MWCNTs) and vanadium oxide (VOx) and an organic electrolyte.[74] (b) Schematics of a free-standing solid-state yarn NiCo//Zn battery. [77]

In addition to the twisted or spring structure, a novel concept for electronic devices architecture—a tube-type devices show superior mechanical flexibility. A heat-shrinkable tube is used to encapsulate the device and provides sufficient pressure for holding all components closely. [78] For instance, the tube-type lithium-ion battery is composited by a hollow helix anode (Ni /Sn -coated Cu wires), a modified polyethylene terephthalate (PET) nonwoven separator and a rigid cathode (**Figure 6a, b**). The fiber shape and omni-directional flexibility of the cable battery make it can be placed anywhere and in any shape. Moreover, the cable battery could be worn on the weaved into different types to meet the requirement of our daily life, which will facilitate the realization of practical wearable electronics. The cable battery shows good charge/discharge

behaviors and stable capacity retention, similar to its designed cell capacity (per unit length of the cable battery) of 1 mA h cm^{-1} under a voltage range of 2.5-4.2 V. [79] With further optimization of the battery components, the cable-type battery will undoubtedly have a great impact on the fields of portable, wearable, and flexible electronics. For its practical use, a commercial light emitting diode was lighted, even though the battery is intentionally bent and spiral. [80] Meanwhile, the yolk- shell NiS_2 @ porous carbon fibers electrode was fabricated by vapor deposition. Tube-type concept was also used to design the flexible fiber shaped sodium ion battery (**Figure 6g, h**). And it exhibited stable performance under different bending conditions. Even at high bending angles of 120 ^{o} and 150°, only 9 % and 11 % of reversible capacity reduction occurred.[81]The graphene/CNT composite fiber also had been applied as electrodes to produce wire-shaped dye-sensitized solar cells with a photoelectric conversion efficiencies up to 8.50% and supercapacitors with a specific capacitances up to 31.50 $F{\cdot}g^{-1}$ (4.97 $mF{*}cm^{-2}$ or 27.1 $\mu F{\cdot}cm^{-1}$), much higher than the bare CNT fibers under the same condition.[82] Based on the concept of self-powering, the application of energy-harvesting technologies from ambient environment for sustainable operation may be the most promising alternative to meet the increasing energy requirement. The explored fiber shaped integrated energy devices attracted much more attention. A novel, all-solid-state, flexible "energy fiber" that integrated the functions of photovoltaic conversion and energy storage has been made on the basis of titania nanotube-modified Ti wire and aligned MWCNT sheet as two electrodes. the "energy fiber" could be bent into various forms depending on the application requirement. And the entire photoelectric conversion and storage efficiency during bending was slightly decreased by less than 10% after bending for 1000 cycles without sealing.[83] In **Figure 6(i-j)** , supercapacitor-triboelectric nanogenerator power system was designed, which can harvest mechanical energy from human motion. In this system, the nanogenerator charge supercapacitor by the contact-electrification and electrostatic-induction process, demonstrating that this self-charging power system is a very promising concept to meet the increasing demands of flexible power sources in wearable electronics.[84, 85]

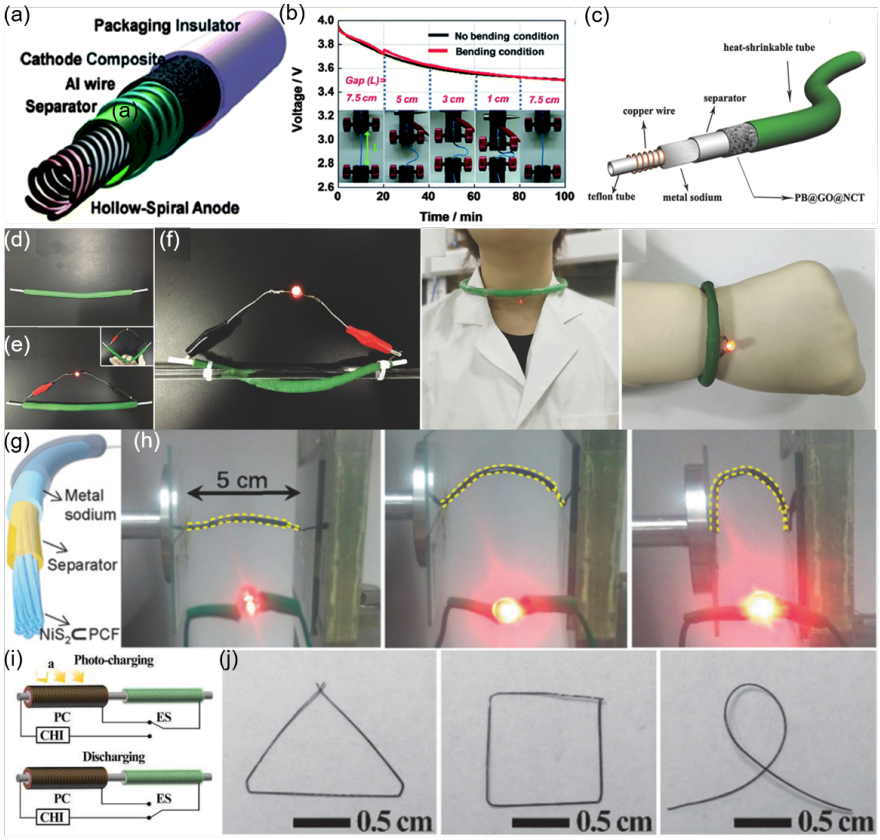

Figure 6 . (a) Schematic illustration of the cable battery with hollow-helix anode having multiple-helix structure. (b) Discharge characteristics with variations in bending strain every 20 min.[79] (c) Schematic illustration for the structure of the tube-type flexible SIBs. (d) Digital photograph of the fabricated tube-type flexible sodium ion battery (SIBs). (e, f) Demonstration of an LED lighting by tube-type flexible SIBs under different conditions.[80] (g) Schematic illustration for the construction structure of the flexible fiber-shaped sodium battery and (h) photos of LEDs lightened by as-assembled fiber-shaped sodium battery under different bending states.[81] (i) Schematic diagram shows the circuit connection state in the process of charging and discharging. (j) Photograph of "Energy fibers" being bent into various shapes.[83]

3. The paper-like wearable electronics

Different from the conventional electrodes prepared via the slurry-coating method, free-standing materials can be utilized directly as electrodes or substrate to support rigid active materials without binder, conductive additive, and even metal current collector.

3.1 Flexible electrodes based on conductive substrate

Up to now, Carbon based materials such as CNTs, graphene, carbon fiber and carbon cloth can be easily assembled into flexible membranes by vacuum filtration, self-assembly, dry-drawing, blade-coating, ink printing. A versatile approach of achieving flexible electrodes is to filter solutions containing nanosized active materials with flexible substrates (CNT, graphene, cellulose, PAN) and other 2D layered material (transition metal dichalcogenides: *e.g.* MoS_2, WS_2). The active materials offer substantial specific capacity, while the CNTs and graphene provides both electronic conductivity and mechanical support. Moreover, surface modifications of the conductive substrates are required to enable solution processing and enhance the electronic conductivity. Flexible electrodes composited by these materials showed impressive electrochemical performances. Researchers mostly focused on finding new electrode materials and unique structure with a highly conductive pathway for electrons, a short ion diffusion length, and a fast transport channel for the ion delivery. Graphene based films have been obtained by spin-coating, layer-by-layer and vacuum filtration. For example, Liu *et al* . reported that a folded structured graphene paper is obtained by freeze-drying, thermal reducing of a GO aqueous dispersion. This paper-like graphene is free-standing and flexible. And the folded structure of the graphene sheets with fewer layers could provide more lithium insertion active sites, such as edge-type sites and nanopores. As electrodes for LIB, it shows first discharge and charge capacity are 1091 and 864 mA h g^{-1}, corresponding to the initial coulombic efficiency 79.2%. [86] Moreover, a graphene-based flexible electrode was applied both to a cathode and anode by employing a pulsed laser deposition technique. A reversible capacity of 21 μAh cm^{-2} was observed for nanostructured V_2O_5/graphene paper, which is significantly improved than that reported previously for thin film electrodes with amorphous V_2O_5.[87] Besides that, ultrathin and flexible graphene paper have been also used for supercapacitor. For instance, a porous graphene film was fabricated by a template method and filtration. PANI nanowire arrays were grown on the surface of the film. This composite film was assembled into a flexible supercapacitor by using Au-coated polyimide film as both current collector and encapsulating material. Base on the CV curves under different bending status, the geometry deformation have no effect on the performance of the flexible devices.[88]

Similarly, Free-standing MWNT thin films was prepared by simple lamination process, electrospinning, weaving, or vacuum filtration, which was used as current collectors for both anode and cathode. In 2007, flexible batteries and supercapacitors based on cellulose paper embedded with CNT and room temperature ionic liquids electrolyte was designed. Unmodified plant cellulose dissolved in RTIL ([bmIm][Cl]) is infiltrated into the MWNT to form a uniform film of cellulose and [bmIm][Cl], embedding the MWNT. After solidification on dry ice and removing excess RTIL and ethanol, the resulting nanocomposite paper forms the basic building unit in those flexible devices. [89] Hu*et al.* also demonstrated that the free-standing, lightweight CNT films were used as the collectors, $Li_4Ti_5O_{12}$ and $LiCoO_2$ slurries were coated on CNT films by a simple lamination

process. And the whole device was sealed with 10 μm PDMS. No failure was observed for the paper battery after manually bending the device down to 6 mm for 50 times. [90] Xiao*et al.* reported a free-standing mesoporous VN/CNT hybrid electrode prepared by vacuum filtration of a solution mixture of vanadium nitride (VN) nanobelts and CNTs. Both VN and CNT have excellent electrical conductivity that ensures its application as electrode without current collectors. CNT and graphene suffer from a large irreversible capacity, low initial coulombic efficiency and fast capacity fading, which are mainly due to the re-stacking structure and side reactions between carbon materials and electrolytes arising from the functional groups and defects of the carbon materials.[91]

To improve the capacity and cycling stability, heteroatoms (N, B, S, P) doping, nanostructured Si, Sn, metal oxides (Co_3O_4, SnO_2, TiO_2, Mn_3O_4, Fe_2O_3, *etc* .) and transition metal dichalcogenides (TMDCs *e.g* ., MoS_2 and WS_2) have been used to modify the free-standing substrates.[92-95] Heteroatom doping with nitrogen, boron could induce a large number of defects, leading to an increase in the reversible capacity,[68, 96, 97] while the nanostructure could accommodate the strain of lithium insertion/extraction, increase the contact area between electrode and electrolyte and short the path lengths for electronic and ions transport.[98] As shown in **Figure7(a-d)** , hierarchical $ZnCo_2O_4$nanowire arrays/carbon cloth exhibits high capacity of 1300 mA h g^{-1}, maintains 96 % of the initial capacity after 40 cycles. The 3D configuration of the composite greatly increases the electrolyte/$ZnCo_2O_4$ contacts area. The loose textile accommodates the strain induced by the volume change during electrochemical reactions. [99] Meanwhile, Various carbon additives have also been mixed with the metal oxide particles to improve their conductivity. For instance, vanadium oxide (V_2O_5) nanowires were synthesized by hydrothermal reaction based on the network of ultra-long CNTs. The composite electrodes with 25 wt.% CNTs show a strength of 4.7 MPa, which is significantly higher than that of CNT and V_2O_5 nanowire electrodes. It also exhibits 318 mAh g^{-1} at the current density of 70 mA g^{-1}.[100] David *et al* . demonstrated synthesis of a composite-layered paper consisting of acid-exfoliated MoS_2 nanoflakes in an rGO matrix with mechanical strength 2–3 MPa and high failure strain (approximately 2%). The electrode stabilized to a charge capacity of 240 mAh g^{-1} at a current density of 25 mA g^{-1} (with respect to total weight of the electrode) after the initial five cycles.[101] Carbon cloth are commonly termed as CC, a highly conductive textile with more superior mechanical flexibility and strength than the graphene, CNTs and cellulose paper, holds a great commitment in serving as a flexible substrate in the fabrication of flexible energy storage devices. To date, Numerous flexible energy storage devices have rapidly emerged, including flexible lithium-ion batteries (LIBs), sodium-ion batteries (SIBs), lithium-O_2 batteries. In **Figure7(e-f)** , a Fe_{1-x} S@PCNWs/rGO hybrid paper was also fabricated by vacuum filtration, which displays superior flexibility and mechanical properties. A flexible packaged full cell is fabricated. As demonstrated, it works well under continuous bending process.[102] Therefore, the flexible potassium-ion batteries (KIBs) comes into being. Highly crystalline Prussian blue (PB) nanocubes was synthesized onto Xuan paper by cyanotype, which is a novel photographic printing strategy. The photographic printing flexible PB cathode and graphite/Cu anode were assembled in a flexible device, which is sealed by Al-plastic film. For practical applications, a LED could be lighted even though the device is intentionally bent and folded (**Figure 7g** and**7h**). And its discharge capacity remains almost unchanged under different geometric deformation (bent and folded).[103,104] Graphene sheets also used to incorporate high storage capacity Si, employing as a stable and self-supporting composite electrode with enhanced accessible interior and high rate capacity.[105-107] By magnesiothermic reduction and layer-by-layer assembly process, an inter-overlapped Si hollow nanosheet and rGO flexible electrode was obtained for flexible LIB (**Figure** 8a and 8b). The Si/rGO films deliver a high specific capacity of 904 mAh g^{-1} at 200 mA g^{-1} and possess an excellent stability (650 mAh g^{-1} after 150 cycles). From the **Figure 8c** , the capacitance is not affected by the deformation of the flexible LIB. [107]

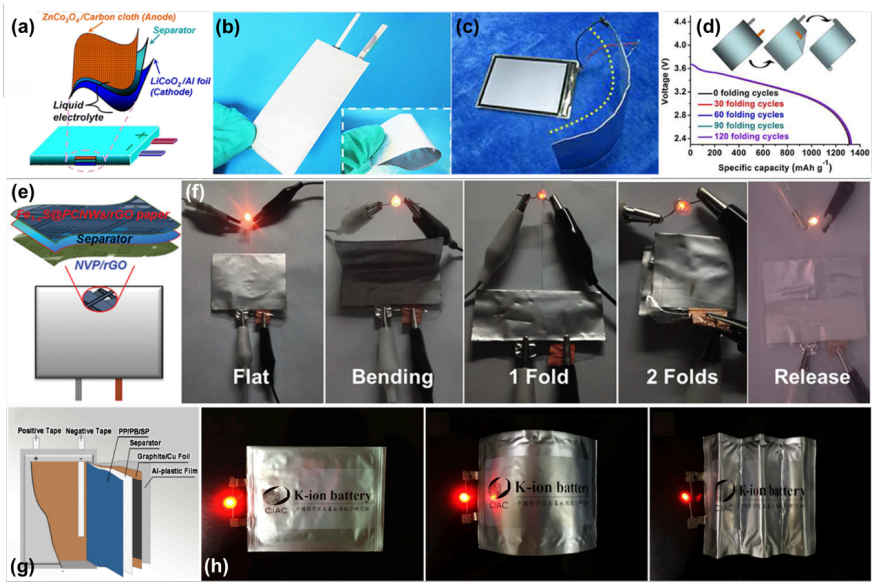

Figure 7. (a) Schematic illustration for the fabrication of the hierarchical 3D $ZnCo_2O_4$ nanowire arrays/carbon cloth/liquid electrolyte/$LiCoO_2$ flexible lithium-ion battery. (b) Photograph of the fabricated flexible Li-ion battery. (c) The digital photo of tuning on a mobile phone screen by a foldable battery. (d) The voltage versus specific capacity profiles of full flexible battery before and after 30, 60, 90, and 120 cycles of bending.[99] (e) Schematic illustration for fabrication of the flexible SIB and its structure. (f) Digital photos of the flexible SIB lightening a LED under various states.[102] (g) Photographs of the fabricated, flexible KIBs. (h) Demonstration of an LED light by flexible KIBs under flat, bending, and folding states.[103]

Compared with secondary rechargeable batteries with volatile and flammable organic electrolytes, aqueous rechargeable batteries are more promising considering the cost and safety as well as the ionic conductivity of electrolyte. The successful realization of the flexibility of such kinds of batteries provides an effective strategy to enrich the family of flexible energy storage systems. Flexible devices such as nickel–metal (*i .e* ., cadmium, iron, zinc, or Bismuth),[38, 108-110] Zn–MnO_2battery,[111-115]alkali-ion battery[116, 117] exhibit high ionic conductivity, environmental issues, good safety, and low cost. Much more efforts have been devoted to developing novelty cheap electrodes with unique nanostructures to meet the flexibility and energy storage requirement.[118-120] Rechargeable Ni-Fe batteries were assembled by direct growth of $Ni(OH)_2$ nanosheets and mesoporous Fe_2O_3 nanorods on the GF/CNTs hybrid films. Two flexible poly(ethylene terephthalate) (PET) sheets were used as flexible substrates. The Ni/Fe cell exhibited an energy density of 100.7 Wh kg^{-1} at 287 W kg^{-1}. Moreover, the cell also shows good cycling stability with capacity retention of 89.1% after 1000 cycles. There was little changes in the charge/ discharge curves at different bending angles (up to 60°).[38] Compared with other aqueous batteries, Ni-Zn battery has a high output voltage. But the cycle stability is usually very poor. The nanostructure can be a cushion of the shape change during charge and discharge and effectively suppress the Zn dendrite growth. It also facilitated electrolyte penetration and fast ion/mass transport. Therefore, ZnO and NiO nanoparticles have been deposited on the 3D network carbon cloth-carbon nanofiber substrate (**Figure 8d**). The full cell quasi-solid-state device showed good suitability to shape deformation and 91.45% capacity retention after 1000 cycles.[121] Li *et al* . designed a solar charged planar flexible quasi-solid-state Ag-Zn battery [**Figure 8(e-f**)]. Carbon cloth coated with Ag nanowires and Zn nanoflakes were used as flexible cathode and anode. Eventually, a flexible device was obtained with KOH-PVA gel electrolyte in a classic sandwich structure. It delivers a capacity of 1.245 mAh cm^{-2}, which hasn't obvious different at various angles from 0 to 135°.[122]

Besides above batteries, an energy storage system based on a battery electrode and a supercapacitor elec-

trode called battery-supercapacitor hybrid (BSH) offers a promising way to construct device with merits of both secondary batteries and SCs. In 2001, the hybrid energy storage cell was first reported by Amatucci. A activated carbon cathode and nanostructured $Li_4Ti_5O_{12}$anode were assembled into the cell.[123] Li-ion BSHs systems with organic electrolytes could work under a wider potential window and hence much higher energy density is obtained. For example, materials used as Li-insertion hosts are, $Li_4Ti_5O_{12}$(LTO)[124], Nb_2O_5[125], V_2O_5[126], $LiMn_2O_4$[127], $Li_3V_2(PO_4)_3$[128]. Aqueous Li-ion BSHs is an attractive hybrid device due to the high safety (nonvolatile, nonflammable, and nontoxicity) and high ionic conductivity of aqueous electrolytes as well as the facile device assembly process. They usually use neutral aqueous lithium-salt solutions (Li_2SO_4, $LiNO_3$, and LiCl, *etc* .) as electrolytes. A high-performance solid-state carbon nanotubes $(CNTs)_{(+)}//Fe_3O_4–C_{(-)}$alkaline battery-supercapacitor hybrid device was constructed, which delivered a volumetric energy density of 1.56 mWh cm^{-3}. This solid-state hybrid device also can withstand mechanical deformation and different environmental temperatures ranging from 20 to 100 degC. [129] Li*et al* . demonstrated that a quasi-solid-state Na-ion BSH was designed using the PVDF-HFP membrane as the matrix of gel electrolyte. The urchin-like $Na_2Ti_3O_7$and activated carbon derived from peanut shell were used as anode and cathode (**Figure 8g**). A high-energy density of 111.2 W h kg^{-1} is achieved at a power density of 800 W kg^{-1}. In addition, the capacity could maintain 86% after 3000 cycles. There is no obvious loss of capacity under different bending (**Figure** .8h). [130][131-136]

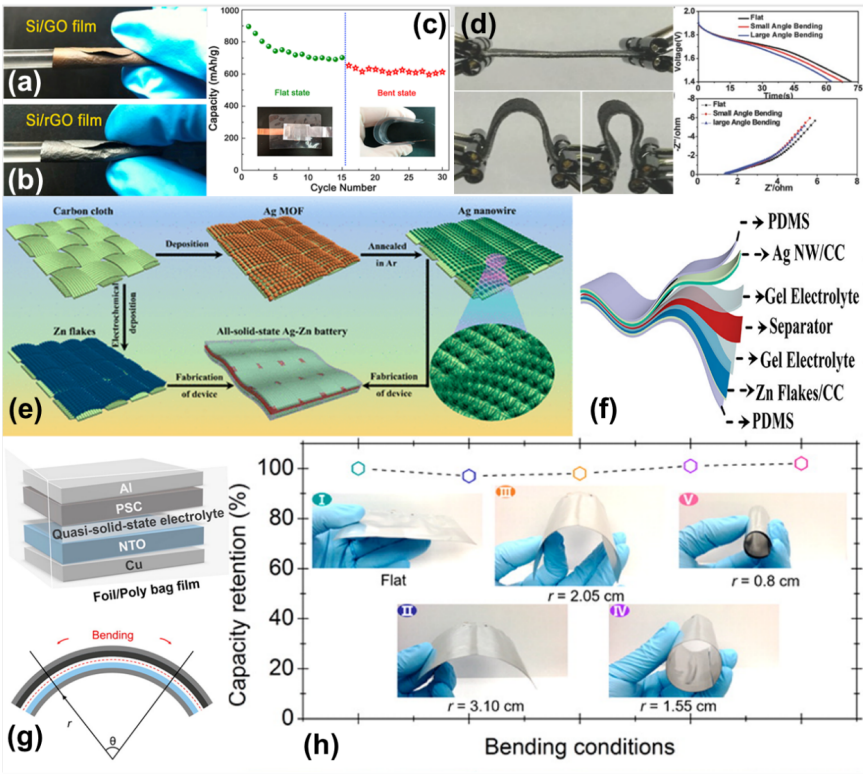

Figure 8 . (a, b) Photos of Si/rGO flexible film in different states; (c) Electrochemical performance of the flexible full LIB for 15 cycles at 50 mA g^{-1} in both flat and bent state. d) Discharge curves and EIS results of flexible quasi-solid-state Ni–Zn battery with different bending conditions. [121]e) Schematic illustration of the synthesis of the flexible quasi-solid-state Ag-Zn battery; f) Schematic diagram of the fabricated flexible quasi-solid-state Ag-Zn battery.[122] g) Schematic illustration of the structure of the quasi-solid-state sodium ion capacitor. h) Stability of capacitive performance of the quasi-solid-state sodium ion capacitor collected at different bending conditions (the inset shows the flexibility with different mandrel radius). [130]

3.2 Flexible electrodes based on nonconductive substrate

As it turns out, the graphene, carbon nanotube and carbon cloth have good film forming property. However, the mechanical performance of pure carbon materials is not sufficient. Therefore, the polydimethylsiloxane (PDMS), cellulose paper, polyethylene terephthalate (PET) and polymethylmethacrylate (PMMA) with superior mechanical performance are introduced to support the active material. Many electronic materials can provide good bendability when prepared in thin-film form and placed on thin substrate sheets or near neutral mechanical planes in substrate laminates.[137-141] In **Figure 9(a-e)** , Sandwich structured flexible device have been fabricated by employing cellulose paper as the flexible supporting layer. It shows superior mechanical property and can undergo severe bending.[141] A graphene-cellulose paper was designed that combined the conductivity and electroactivity of graphene and excellent mechanical property of cellulose paper. It presented a stress of 8.67 MPa and an elongation of 3%, which is much more superior than the pure graphene paper. [139] PPy, PANI, PEDOT, PSS, PMT and other conductive polymers were usually used to enhance the conductive of insulated and flexible substrate such as cellulose paper, PDMS, PTFE membrane. [142-144] A low temperature hydrothermal method was used to fabricate piezoelectric nanogenerator. ZnS-NRs and conducting filler (PANI or MWCNTs) were dispersed in PDMS matrix to form a composite film. The geometric deformation (rolling, twisting, folding and bending) demonstrate the flexibility of the flexible piezoelectric nanogenerator [**Figure 9(f, g**)]. Furthermore, this device is tested for wireless detection of pressure impact (13.6 kPa) in terms of output voltage/response. This application can be demonstrated by integrating a piezoelectric nanogenerator, infrared LED, photodiode and a digital oscilloscope.[145] CNF/PDMS aerogel film was obtained by freeze-drying, sandwiched between two thin PDMS films and aluminum foils, to form the flexible piezoelectric nanogenerators. Under the periodic external mechanical stimulate, the output signal is stable and high. [146] Patterned PDMS also used as supporting layer of an array of GaAs for stretchable inorganic photovoltaic devices. [147] An ultrathin, light, and flexible organic photovoltaic device was constructed on polyethylene terephthalate (PET) substrates. It showed extreme mechanical resilience, which survive quasi-linear compression to below 70% of their original area. [3]

In the **Figure 9(h-k)** , a microfluidic system was constructed on flexible and patterned PDMS substrate with reagents for colorimetric analysis. This bioelectronic can maintain the structure under the geometric deformation (stretching, bending and twisting).[148] Although these systems show significant functions, they couldn't make a real impact in our lives. It is difficult to build a long-period, strong electrical contacts without irritation of the electronic skin and achieve integrated systems with different electronic elements that do not cause discomfort during prolonged use. Indeed, skin can be regarded as a signal source: It can both generate and transmit biological signals that provide important health metrics of an individual. Researches inspired by this multifunctional biological model have been developing large-area networks of sensors that can detect pressure, temperature and other environment stimuli. Organic and inorganic materials have been used to fabricate artificial electronic skins. A variety of sensors (e.g., mechanical [149, 150] and temperature sensors[151, 152]) integrated on plastic and/or elastomeric substrates can capture signals, simulating mechano- and thermo-receptor properties of skin tissues. Toward this end, multifunctional sensors (temperature, strain, and electrophysiological), microscale light-emitting diodes (LEDs), circuit elements (such as transistors, diodes, and resistors), wireless power coils, and high-frequency inductors, capacitors, oscillators, and antennae, all integrated on the surface of a thin (~30 μm), gas-permeable elastomeric sheet based on a modified polyester (BASF, Ludwigshafen, Germany) with low Young's modulus (~60 kPa). As shown in **Figure 9(l-p)** , the devices and interconnects exploit ultrathin layouts (<7 μm), neutral mechanical plane configurations, and optimized geometrical designs. The active elements use established electronic materials, such as silicon and gallium arsenide, in the form of filamentary serpentine nanoribbons and micro- and nanomembranes. The result is a high-performance system that offers reversible, elastic responses to large strain deformations with effective moduli (<150 kPa), bending stiffnesses (<1 nN m), and areal mass densities (<3.8 mg/cm^2) that are orders of magnitude smaller than those possible with conventional electronics or even with recently explored flexible/stretchable device technologies.[153]

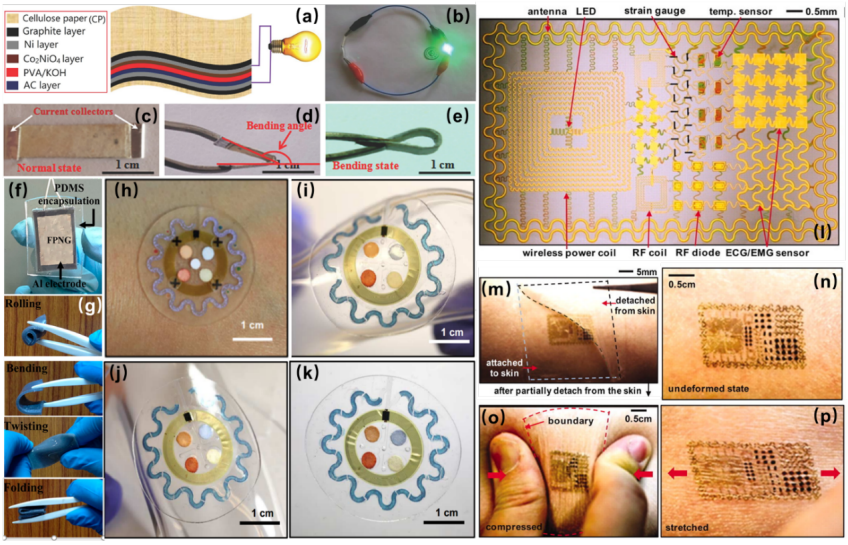

Figure 9 . (a) Schematic illustration for the assembled graphite/Ni/Co_2NiO_4-CP//graphite/Ni/AC-CP ATFSCs; (b) A light-emitting diode (LED) powered by 2 ATFSCs in series; The flexible assembled ATFSCs: (c) normal state, (d,e) bending states.[141] (f) A digital photographic image of PDMS encapsulated PZP-FPNG with Al electrodes. (g) The flexibility of the PZP-FPNG is demonstrated by rolling, twisting, folding and bending states.[145] (h) Optical image of a fabricated device mounted on the forearm. (i-k) FEA results of stress distribution associated with the devices on phantom skin (PDMS) and respective optical images under various mechanical distortions: stretching at 30 % strain, bending with 5 cm radius, and twisting.[148] (l) Image of a demonstration platform for multifunctional electronics with physical properties matched to the epidermis. Mounting this device on a sacrificial, water-soluble film of PVA, placing the entire structure against the skin, with electronics facing down, and then dissolving the PVA leaves the device conformally attached to the skin through van der Waals forces alone, in a format that imposes negligible mass or mechanical loading effects on the skin. (m) EES partially peeled away from the skin. Multifunctional EES on skin: undeformed (n), compressed (o), and stretched (p).[153]

4. The 3D network electrode

Currently, 3D electroactive nanostructured materials grown directly on conductive substrates as binder-free integrated electrodes for batteries is an emerging new concept, which can not only avoid the "dead surface" in conventional slurry painted electrodes and allow for more efficient electron transport but also simplify electrode fabrication. Here, we just discuss the 3D materials which is stretchable and compressible on the micro and macro aspects. 3D porous frameworks possess multidimensional electron transport pathways, easy access to the electrolyte, and minimized transport distances between bulk electrode and electrolyte. Recently, significant research efforts have been focused on three-dimensional (3D) interconnected network (such as aerogels, hydrogels and foams) as current collector or matrix and scaffolds via hydrothermal, layer-by-layer assembly and chemical vapor deposition methods.

Chen and his co-workers first synthesized graphene foam by the CVD method [**Figure10(a-b)**].[154] After combining with PDMS, the obtained free-standing graphene foam (GF) is extremely light and flexible with high conductivity. And the resistance of the GF/PDMS composite became stable after several cycle of bending or stretching. This composite also showed a shielding effectiveness of 30 dB in the 30 MHz-1.5 GHz frequency range and 20 dB in the X-band frequency range. More importantly, the specific EMI shielding effectiveness can reach 500 dB cm^3g^{-1}. No obvious performance degradation is observed under the mechanical

deformation. [155] Inspired by this work, the similar 3D structured materials showed great potential application of nanogenerators, supercapacitors and other energy storage systems. [156-159] Typical 3D structured aerogels and hydrogel could be easily obtained by the reduction of a graphene oxide dispersion, in which flexible graphene sheets partially overlap in 3D space to form interconnected porous microstructure. This unique hierarchical architecture not only prevents serious restacking of graphene sheets but also allows electrolytes to freely diffuse inside and through the network. Therefore, a free-standing electrode was constructed by a thickness of 3 mm graphene hydrogel supported by gold coated polyimide substrate. Flexible supercapacitor was assembled by employing H_2SO_4-PVA as solid-state electrolyte. The change of CV curves under different bending angles at the scan rate of 10 mV s^{-1} is negligible.[160] In **Figure 10(c-d)** , the 3D hierarchically nanostructured hydrogel was synthesized by a facile interfacial polymerization method in which the polymerization is carried out at an organic/aqueous biphasic interface. The microstructure of the PPy hydrogel and its mechanical and electrochemical properties could be tuned by controlling the ratio of phytic acid to pyrrole monomers in the synthetic process.[161] Qu *et al.* reported a compressible supercapacitor [**Figure 10(e-g**)], which is fabricated by hydrothermal treatment and electro-polymerization. The obtained PPy-G foam can sustain large-strain deformation under manual compression and recover most of the material volume. From the CV and GCD (charge and discharge) curves, the compressible supercapacitor could output stable energy with different compressive strain.[162] PANI/Ag/CNF aerogel was synthesized by situ-reduction and electrodeposition. It can deliver a capacitance of 176 mF cm^{-2}. The specific capacitance shows almost no change under different bending radius.[163] In addition, 3D electronics are mostly employed in electrons signaling, stimulation, and electrically triggered-response devices. For bioelectronics, BSA–rGO hydrogel electrode was fabricated *via* photopolymerization, which is demonstrated to be a highly effective H_2O_2 biosensor electrode with low detection concentration and high sensing sensitivity after combining with hemin chloride. [164] Inspired by the adhesion behavior of mussels, a PDA-pGO-PAM multiple network hydrogel was developed, possessing high toughness and conductivity as well as self-adhesiveness and self-heapability. The hydrogel had good self-adhesiveness to skin tissue and used as a motion sensor self-adhered on a human body to to detect the electromyographic signal (EMG) during the relaxation tension of arm. It also was cyto-compatible for regulating cell behaviors, indicating plausible therapeutic applications. [165] Jaemin demonstrated smart prosthetic skin instrumented with ultrathin, single crystalline Silicon nanoribbon strain, pressure and temperature array sensors.[149] The silicon nanoribbon (SiNR) was designed as unique serpentine geometry to stretch according to the dynamic mechanical properties of the target skin segment. This design strategy provided the highest levels of spatio-temporal sensitivity and mechanical reliability, thereby dramatically enhancing the perception capabilities of artificial skin in response to highly variable external environments. This collection of stretchable sensors and actuators facilitate highly localized mechanical and thermal skin-like perception in response to external stimuli, thus providing unique opportunities for emerging classes of prostheses and peripheral nervous system interface technologies. To truly simulate human skin, Electronic skin should be able to emulate the touch and pressure sensitivity of human skin embodying a duality of being able to recognize both medium pressure (10–100 kPa, suitable for object manipulation) and low pressure (<10 kPa, comparable to gentle touch) perturbations.[150] 15 nm thick layer of sputtered a-IGZO, 25-nm thick Al_2O_3 passive layer were macro machined on the top of a 1 μm thick parylene film. The transparent device exhibits a mobility of 11 cm^2 V^{-1} s^{-1} andI_{on}/I_{off} greater than 10^4, which also could withstand bending radius of 50 μm and can pave the way to ultra-flexible and transparent displays. To design a concrete application, it could be used to monitor the intraocular pressure for glaucoma. [166] For human skin in robotic and prosthesis applications, slip is an important information to grab an object.[167] To address simultaneously the slip force, tactile force, and temperature, a macroscale printing fabrication technique was used to prepare a strain-engineered three-axis tactile force sensor and temperature sensor array. The flexible device can detect three-axis force and the temperature sensitivity is 0.25% /°C. Similarly, human skin can feel moving air without touching physically, the device can detect the N_2 gas with a source pressure of 0.2 MPa. Lucie[37] also prepared a soft tactile sensor using two textile electrodes, a non-stretchable copper/tin coated textile. The flexible sensor presented minimal detectable weight and displacement is 10 mg and 8 μm within a wide normal force range (potentially up to 27 N (400 kPa)) and natural touch-like tangential force ranges (from about 0.5 N to 1.8 N). Qu*et al.* reported a compressible supercapacitor, which is fabricated

by hydrothermal treatment and electro-polymerization. The obtained PPy-G foam can sustain large-strain deformation under manual compression and recover most of the material volume. From the CV and GCD (charge and discharge) curves, the compressible supercapacitor could output stable energy with different compressive strain.[162] Except the compression deformation, an stretchable supercapacitor with good tackiness was fabricated based on the cross-linked polyacrylamide(PAM) networks soaked by EG/Water/H_2SO_4. PANI was in-*situ*grown onto both sides of the above organohydrogel polyelectrolyte [**Figure 10(e-f)**]. It warrants a high structural integrity and stable electrical conductivity under stretched states. Due to the interconnected polymer network, the external force could be evenly dissipated without causing interfacial separation between the electrode and the electrolyte (**Figure 10i**). With this integrated structure, the device shown a stable energy output under bending, twisting and stretching states [**Figure10(h-j)].** [168]

Additionally, devices took advantages of human movement such as touching, impact, linear sliding, rotation, and vibration to produce electricity attracted much more attention.[169-177] The flexible piezoelectric thin film NG on a single thin plastic substrate converted a high-output performance of 200 V and 150 μA·cm^{-2} from the slight mechanical deformations. The short-circuit current generated from a large-area NG (3.5 cm x 3.5 cm) reached up to 8 μA and readily allowed more than 100 commercial blue LED arrays to operate during slight bending motions by human fingers. [170] For instance, J. M. Donelan developed a biomechanical energy harvester that generates electricity during human walking. The energy harvester mounts at the knee and selectively engages power generation at the end of the swing phase, thus assisting deceleration of the joint. When walking with one device on each leg, it produced an average of 5 watts of electricity.[178]

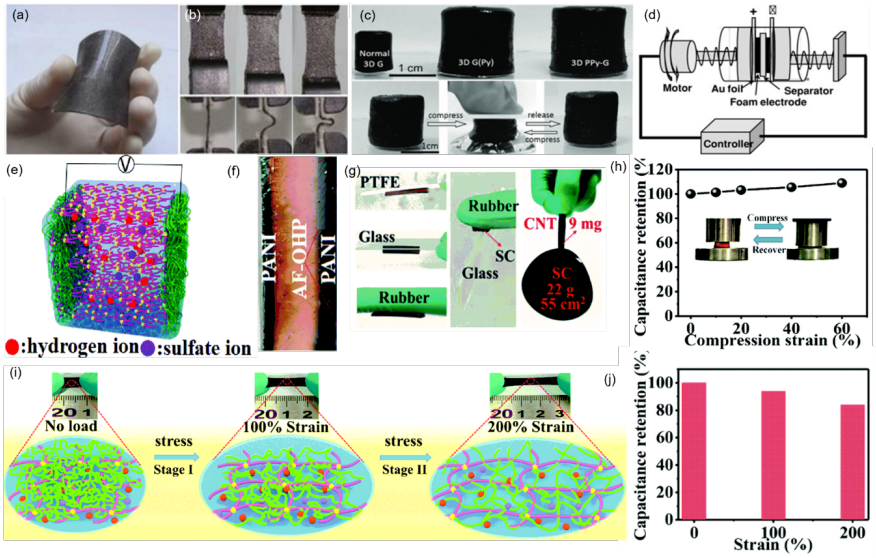

Figure 10. (a) Photograph of a bent GF/PDMS composite, showing its good flexibility. (b) the stretching and bending process of GF/PDMS.[154] Flexible PPy hydrogel-based supercapacitors: (c) EIS curve of a full cell based on symmetric electrodes. Inset: schematic of the makeup of the flexible supercapacitor. (d) CV curves of the fabricated supercapacitor under different bending conditions at a scan rate of 100 mV s^{-1}.[162] (e) Mechanism diagram and (f) optical picture of cross-section of AF-SSC. (g) Optical picture SCs adhered to different substrate surfaces. (h) Capacitance retention of AF-SSC under different stretch ratio of AF-SSC. (i) Schematic illustration of the stretching process (j) Capacitance retention of AF-SSC at the current density of 0.2 mA cm^{-2} under different compress ratio.[168]

5. Flexible electrolytes

For batteries, Liquid electrolytes have played vital roles in energy storage devices for several decades, which allow Li^+, Na^+ and K^+ to diffusion between anode and cathode. Commonly, $LiPF_6$, $NaClO_4$ based liquid electrolyte are used in the most of previous reports. However, liquid electrolytes are in danger of leakage and even combustion of organic electrolytes. It is also likely to induce short circuit of battery when it was assembled improperly, resulting in fire or explosion of the cells. Another disadvantage of liquid electrolytes is the inevitable alkaline metal dendrite growth in half and full cell, which is caused by uneven currents when charged in the case of porous separators. In addition, the liquid electrolyte is reducible on the anode side and solid electrolyte interphase (SEI) is formed during charge and discharge process, leading to the loss of ionic (*e.g* . Li^+, Na^+, K^+) from the cathode and lower initial coulombic efficiency. Replacing the organic electrolytes in different kinds of batteries with ceramic electrolyte and polymer electrolyte, which are intrinsically nonflammable, to assemble all-solid-state batteries has the promise to ultimately resolve the safety issue.

5.1 Polymer electrolytes

Normally, a solid electrolyte should have high ionic (*e.g* . Li^+, Na^+, K^+) and low electronic conductivity, wide and excellent electrochemical stability window, and chemical compatibility with the electrodes and other components of batteries. In conformity with these rules, various inorganic and polymeric electrolytes have been designed. They are generally composed of polymer matrix and liquid electrolyte, are widely used in alkaline-ion batteries owing to their excellent ionic conductivity, low rates of safety failure, and mechanical flexibility.[179] The macromolecule materials and polymerizable monomers have been used to achieve solid-state electrolyte with a certain mechanical strength.[11, 180] To this end, polymer electrolytes which integrated both advantages of liquid electrolyte and solid electrolytes, have attracted much more attentions as they can function as electrolytes and separators.

Poly (ethylene oxide) (PEO) based polymeric electrolytes have been the most extensively studied polymer systems. Wright *et al.*demonstrated the complexes of Alkali metal ions with PEO. As known, PEO is a semicrystalline polymer whose glass transition temperature and melting point are around 60 °C and 65 °C, respectively. Close to the melting point, PEO becomes soft, promote Li^+diffusion. A lithium polymer salt (LiPSsTFSI) has been synthesized by free radical polymerization. After blending with PEO, the polymer electrolyte exhibits a high ionic conductivity of 1.35×10^{-4} S cm^{-1} at 90 °C but only 6.92×10^{-5} S cm^{-1} at 70 °C. This would be identified as the unique structure of the $–SO_2$-$N^{(-)}$-$SO(=NSO_2CF_3)$-CF_3in the polyanion with high dissociation of Li^+ ions and enhanced the degrees of amorphous phases and the segmental motions.[181]

Besides, single Li-ion conducting solid polymer electrolytes focused on anionic centers (carboxylate ($–CO_2$), sulfonate ($–SO_3$), or sulfonylimide ($–SO_2N^{(-)}SO_2$-, $-SO_2N^{(-)}SO_2CF_3$) anions) have been investigated intensively. Particularly, weakly coordinating anions with a flexible molecular structure (e.g., bis(trifluoromethanesulfonyl)imide ($[(CF_3SO_2)_2N]$, TFSI)) were primarily suggested as requisite counter anions of lithium salt. Cui *et al* prepared an polymer-polymer composite electrolyte (**Figure 11a, b**) with nanoporous polyimide (PI) film filled with polyethylene oxide/lithium bis(trifluoromethanesulfonyl)imide (PEO/LiTFSI).[182] The PI film is incombustible and strong, preventing batteries from short-circuiting. The vertical channels with infused polymer electrolyte could enhance the ionic conductivity (2.3×10^{-4} S cm^{-1} at 30 degC) of the composite electrolyte. The solid-state lithium-ion batteries fabricated with PI/PEO/LiTFSI solid electrolyte show good cycling performance (200 cycles at C/2 rate) at 60 degC and withstand harsh tests such as bending, nail penetration and cutting [**Figure 11(c-e**)]. Other salts and polymer have been designed to resolve these problems. [183, 184] For instance, Lee *et al* . also prepared a highly bendable plastic crystal composite electrolyte (PCCE), which is composed of UV-crosslinked ethoxylated trimethylolpropane triacrylate (ETPTA) polymer network, PVdF-HFP and lithium bis-trifluoromethanesulfonimide in succinonitrile (**Figure 11f**). The S-PCCE provide excellent ionic conductivities of more than 10^{-3} S

cm^{-1} at room temperature and strong resistance to breakage by incorporation of the UV-cured ETPTA polymer network. Notably, the S-PCCE can preserve its dimensional stability even after the 100th bending cycle (**Figure11g**).[185] Wei *et al.* prepared a flexible all-solid-state battery with thin polyethylene glycol electrolyte which could bend to a 1 mm radius with capacity of 0.02 mA h cm^{-2} over 100 cycles.[186] A melamine–terephthalaldehyde–lithium complex (MTF–Li) based single ion conducting electrolyte was designed as the precursor of polymer electrolyte. Then the material was blended with a PVDF–HFP binder and solution cast on a glass dish to form a single ion conducting electrolyte membrane. The tensile strength of the membrane was found to be 3.75 MPa with 31% elongation. The inherent porosity of the material facilitates the accommodation of organic solvents used in battery devices, leading to a high Li ion mobility with an ionic conductivity in the order of 10^{-4} S cm^{-1} at room temperature. [187] Wang *et al.* also demonstrated a double network gel with liquid electrolyte. The gel electrolyte shows a conductivity of 8.1×10^{-4}S cm^{-1} at 30 degC, and it increases to above 10^{-3} S cm^{-1} with an increase of temperature.

In addition, Several kinds of solid state electrolytes such as PVA–KOH, cellulose–chitin–AMImBr–H_2SO_4, PVA–H_2SO_4, PMMA–EC–PC–TEAClO_4 and PAA–KCl, graft copolymer POEM-*g*- PDMS doped with $LiCF_3SO_3$, poly(methyl methacrylate) networks solvated by the ionic liquid EMI.TFSI, have been reported because of high reliability without leakage of electrolyte as well as thin-form and separator-free devices.[188-191]

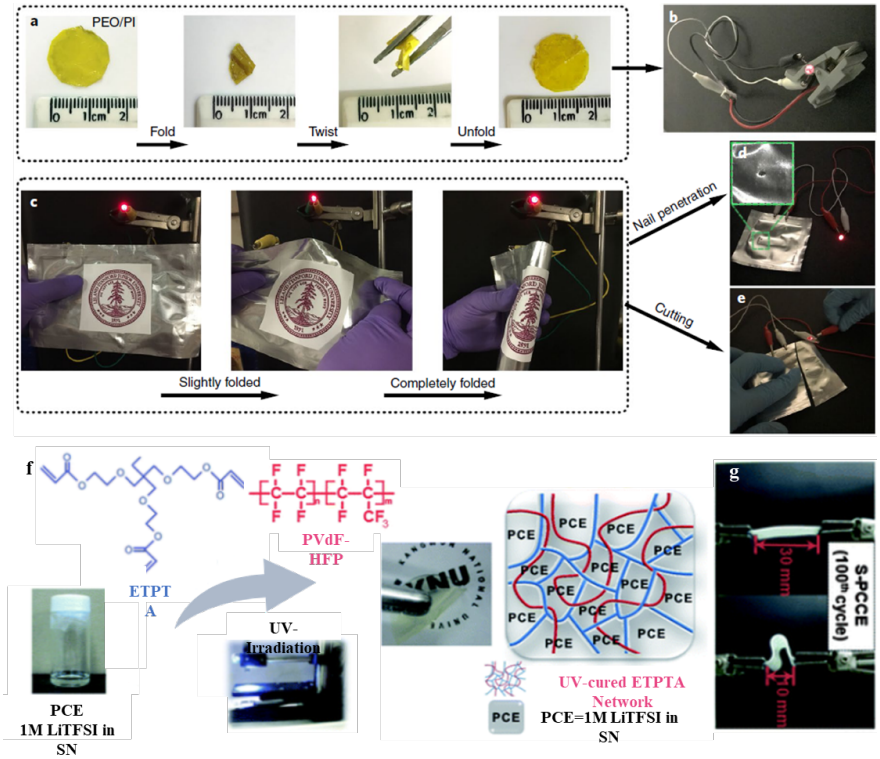

Figure 11. The obtained PI/PEO /LiTFSI polymer-polymer solid-state electrolyte (SSE). (a) Photo images of 2 cm^2 PI/PEO/LiTFSI SSE free-standing film being abused via folding, twisting and unfolding. (b) Photo image of the abused PI/PEO/LiTFSI film as an SSE in a LFP/PI/PEO/LiTFSI/Li coin cell lighting a LED bulb. (c) Flexible Li/PI/PEO/LiTFSI/LFP pouch cell lighting a LED bulb. (d) Li/PI/PEO/LiTFSI/LFP pouch cell lighting a LED bulb after nail test. (e) Li/PI/PEO/LiTFSI/LFP pouch cell lighting a LED bulb after cutting.[182] (f) The schematic representation illustrating the UV-curing process and photographs depicting the physical appearance of S-PCCE. (g) Mechanical bending test of S-PCCE after 100th bending cycles.[185]

5.2 Ceramic electrolytes

Different from the polymer electrolyte, Inorganic ceramic electrolytes have high ionic conductivity (10^{-4}-10^{-3} S cm^{-1}) at ambient temperature. And it also has sufficient electrochemical stability and better flame resistance. As the solid-state batteries became research hotspot again, ceramic electrolyte has achieved significant progress.

In 2016,Kanno reported an sulfides superionic conductor with high conductivity (25mS cm^{-1}) and stability. But the narrow electrochemical stability window, poor chemical compatibility with electrodes, and poor mechanical properties need to be settled urgently. Compared with sulfides (e.g., Li_2S–P_2S_5 and $Li_{10}GeP_2S_{12}$), ceramic oxides (e.g., $Li_7La_3Zr_2O_{12}$and $Li_{1.3}Al_{0.3}Ti_{1.7}(PO_4)_3$) are generally more stable in ambient air and thus can be more easily handled during processing. In particular, the garnet-type $Li_7La_3Zr_2O_{12}$(LLZO) has attracted tremendous interest as a promising solid electrolyte due to its high ionic conductivity (about 10^{-3} S cm^{-1} at 25 °C) and high chemical stability against metallic Li. Kanamura *et al* obtained a flexible composite garnet-type Al-LLZO tape by tape casting and ionic liquid (IL) impregnation. As shown in the **Figure 12a** , the ionic liquid can not only bond the LLZO particles, forming a lithium ions pathway, but also wet the interface of solid-state electrolyte and electrode, reducing the interface resistant. The sheet electrolyte can be casted on the PET substrate and removed easily after drying (**Figure 12b** and**12c**). The sheet electrolyte is mechanically robust, highly conductive (1×10^{-4} S cm^{-1} at 25 degC).[192] With the binder of polytetrafluoroethylene (PTFE), a 3D $Li_{6.75}La_3Zr_{1.75}Ta_{0.25}O_{12}$(LLZTO) self-supporting framework is prepared through a simple grinding method without any solvent (**Figure12e**).[193] Subsequently, a garnet-based composite electrolyte is achieved through filling the flexible 3D LLZTO framework with a succinonitrile solid electrolyte. Due to the high content of garnet ceramic (80.4 wt.%) and high heat-resistance of the PTFE binder, such a composite electrolyte film with nonflammability and high processability exhibits a wide electrochemical window of 4.8 V versus Li/Li^+ and high ionic transference number of 0.53. The continuous Li^+ transfer channels between interconnected LLZTO particles and succinonitrile, and the soft electrolyte/electrode interface jointly contribute to a high ambient-temperature ionic conductivity of 1.2 x 10^{-4} S cm^{-1} and excellent long-term stability of the Li symmetric battery.

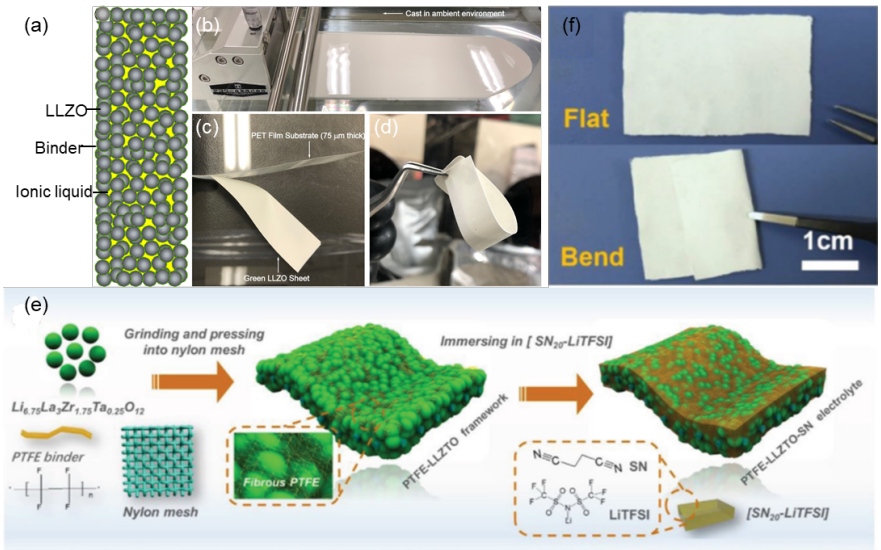

Figure 12. Concept of the flexible composite Al-LLZO sheet electrolyte and its synthesis at room temperature. (a) Illustration of the composite sheet electrolyte, (b) Doctor-blade casting of the sheet electrolyte in ambient air, (c) As-cast green sheet, and (d) Cold-pressed and IL-impregnated Al-LLZO sheet electrolyte.[192] (e) The preparation schematic of 5PTFE-100LLZTO-16[SN20-LiTFSI] electrolyte. (f) Flat and bend state of 5PTFE-100LLZTO-16[SN20-LiTFSI] electrolyte.[193]

5.3 Polymer and Ceramic hybrid electrolytes

Hybrid electrolytes possess the merit of polymer electrolytes and inorganic ceramic electrolytes exhibit comparable ionic conductivity, high mechanical strength, and favorable interfacial contact with electrodes, which greatly improve the electrochemical performance of all-solid-state batteries. [194] It is significant to integrated ceramic electrolyte with polymer electrolyte to endow electrolyte with high ionic conductivity and good mechanical properties, creating a "ceramic in polymer" (CIP) or "polymer in ceramic" (PIC) materials.

The ceramic particle fillers are dispersed into polymer matrix to enhance ionic conductivity. A sandwich-type composite electrolyte was fabricated by a PIC-5 μm interlayer sandwiched between two CIP-200 nm thin layers. The effect of various content and different particle sizes of LLZTO on the conductivity was investigated. Cui and his*co* -workers demonstrated that 15 wt.% $Li_{0.33}La_{0.557}TiO_3$nanowire was dispersed in Polyacrylonitrile-$LiClO_4$, which exhibits an unprecedented ionic conductivity of 2.4×10^{-4} S cm^{-1} at room temperature, suggesting that ceramic nanowire fillers can facilitate the formation of ionic conduction networks in polymer-based solid electrolyte. In addition, the composite electrolyte also shows an enlarged electrochemical stability window in comparison to the one without fillers. The discovery paves the way for the design of solid ion electrolytes with superior performance. [195] In**Figure 13(a, b)** , A 30-50 μm thickness flexible LLZO-PEO ($LiClO_4$) composite electrolyte was prepared by solution-casting method. And the Li ions pathway was investigated systematically. The Li ions mainly pass through LLZO ceramic particles, not the interface or the the PEO polymer. [196]John B. Goodenough and his co-workers also designed a CPMEA/LATP/CPMEA sandwich electrolyte. In the architecture, the ceramic layer (LATP) can block anion transport, which reduces the double-layer electric field at the Li/polymer interface and the decomposition of the polymer electrolyte to improve the coulombic efficiency of a device. The polymer electrolyte layer which is in direct contact with electrodes can suppress dendrite nucleation due to the uniform Li^+flux on the polymer/lithium interface and better wetting ability toward lithium metal. [197] With the PEO as the binder, an ionic liquid (BMP-TFSI) modified flexible concrete structured composite solid electrolyte membrane was obtained (**Figure13c**). The as-prepared membrane is free-standing and exhibits excellent ductility and flexibility. And no cracks could be found in the electrolyte films upon bending, indicating an excellent mechanical capability (**Figure13d**). The addition of the ionic liquid (BMP-TFSI) can not only improve the ionic conductivity, but also enhance the interface stability, suppressing the Li dendrite growth (**Figure 13e**). With the PBL-CSE membrane was used as separator, the solid-state pouch cell presented greatly improved electrochemical performance, thermal stability, and good compatibility toward the Li metal electrode. It can light up a red lightemitting diode (LED) even with folded and corner cut off (**Figure 13f-h**). The effect of particle size and concentration on the strength, ionic conductivity, and interfacial flexibility of composite electrolyte was also investigated. In**Figure** 13i and j, a sandwich type composite electrolyte was fabricated by blade casting with a mechanically strong PIC interlayer and flexible CIP outer layer. Such SCE achieve both excellent Lithium dendrite suppression and interfacial contact with Li metal (**Figure 13k**). Except above active filler (e.g., Li_3N[198] and $Li_{1.3}Al_{0.3}Ti_{1.7}(PO_4)_3$[199]), the inactive filler such as Al_2O_3 have been widely used.

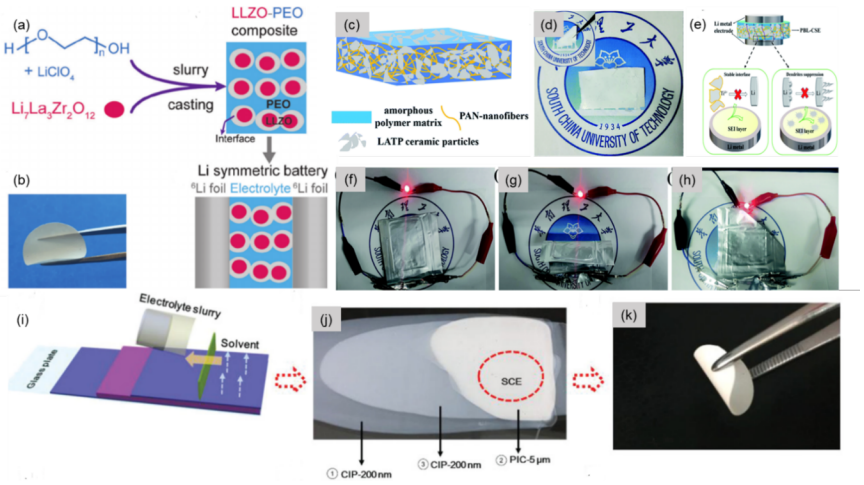

Figure 13. (a) Illustration of the process for preparing LLZO-PEO composite electrolytes. (b) Picture of the as-synthesized flexible composite electrolyte. [196] (c) Schematic illustration of the structure and Li-ion transport mechanism of the PBL-CSE membrane. (d) Digital photograph of the PBL-CSE membrane in the unfolded and bent state (inset). (e) The schematic illustration for the mechanism behind the outstanding Li dendrite suppression ability and superior interface stability against Li metal. (f) Images of the flexible $LiFePO_4$/PBL-CSE/Li pouch Li metal cell lighting a LED bulb even with folding (g) and the corner cut off (h).[200] (i) The schematic illustration of the SCE preparation by blade casting. Digital images of as-casted SCE on a glass plate (j) and the bendable SCE (k).[201]

6. Conclusion and outlook

In summary, flexible rechargeable batteries, supercapacitors, nanogenerators, bioelectronics have been assembled to get robust mechanical stability under frequent mechanical strain, while maintaining excellent electrochemical performance (*i.e* . high capacity, high efficiency, and long cycle stability). However, numerous technical challenges still hinder the development of the flexible devices. New concept of electronic devices will be designed to meet the mechanical flexibility requirement. The wire or planar structure with omnidirectional flexibility (*e.g.* stretch, twisting, compress, bend) is identified as a promising device, which can be weaved into fabric, facilitate rapid growth of wearable electronics.

Additionally, the flexibility of each component is critical for the development of high-performance flexible devices. For electrodes, great progress has been made on high-capacity anode materials. But flexible cathode materials based on $LiCoO_2$, $LiMn_2O_4$, $LiNi_{1/3}Mn_{1/3}Co_{1/3}O_2$ *etc* ., are rarely reported. Therefore, the next stage for flexible electrode will mostly focus on flexible cathode material. Much more effort will be applied for flexible lithium ion and sodium ion batteries.

In terms of the flexible electrolyte, the development of solid-state electrolytes with higher ionic conductivity and larger operating voltage windows is a significant trend in the future. And the interface between electrolytes and electrodes should pay more attention because the different elastic modulus of the electrolytes and electrodes. To get a stable interface between electrolyte and electrodes, a composite electrolyte (CIP or PIC) should be designed with excellent interfacial flexibility and high ionic conductivity. And it not only can suppress the growth of Li dendrite, but also can suppress the growth of Li dendrite.

To further explain and analyze the devices performance during bending or twisting process, advanced simulation methods should be used to build the connection between the mechanical and electrochemical performance and understand the mass transport and electrochemical processes related to the flexible batteries

under external mechanical forces, which is critical to the rational design of new configurations with high performance and flexibility.

Finally, to fulfill the requirements of electronic equipment in the future, it is necessary to fabricate flexible batteries with multiple functions such as optical transparency and tensile and mechanical wear resistance. The combination of flexible batteries with other electronic products such as supercapacitors, sensors and nanogenerators must not be overlooked. And self-powered system will attract much more attention.

References

[1] K. Nomura, H. Ohta, A. Takagi, T. Kamiya, M. Hirano and H. Hosono, *Nature* . **2004** , 432, 488.

[2] G. Gustafsson, Y. Cao, G. M. Treacy, F. Klavetter, N. Colaneri and A. J. Heeger, *Nature* . **1992** , 357, 477.

[3] M. Kaltenbrunner, M. S. White, E. D. Głowacki, T. Sekitani, T. Someya, N. S. Sariciftci and S. Bauer, *Nat. Commun* .**2012** , 3, 770.

[4] B. Y. Ahn, E. B. Duoss, M. J. Motala, X. Guo, S.-I. Park, Y. Xiong, J. Yoon, R. G. Nuzzo, J. A. Rogers and J. A. Lewis,*Science* . **2009** , 323, 1590-1593.

[5] L. Shen, G. Lan, L. Lu, C. Ma, C. Cao, C. Jiang, H. Fu, C. You, X. Lu, Y. Yang, L. Chen, M. Liu and C.-L. Jia, *Adv. Sci.***2018** , 5, 1870077.

[6] Y. Liu, K. He, G. Chen, W. R. Leow and X. Chen, *Chem. Rev.* **2017** , 117, 12893-12941.

[7] A. M. Gaikwad, A. M. Zamarayeva, J. Rousseau, H. Chu, I. Derin and D. A. Steingart, *Adv. Mater.* **2012** , 24, 5071-5076.

[8] M. Yousaf, H. T. H. Shi, Y. Wang, Y. Chen, Z. Ma, A. Cao, H. E. Naguib and R. P. S. Han, *Adv. Energy Mater.* **2016** , 6, 1600490.

[9] G. Nyström, A. Razaq, M. Strømme, L. Nyholm and A. Mihranyan,*Nano Lett.* **2009** , 9, 3635-3639.

[10] R. Bouchet, S. Maria, R. Meziane, A. Aboulaich, L. Lienafa, J.-P. Bonnet, T. N. T. Phan, D. Bertin, D. Gigmes, D. Devaux, R. Denoyel and M. Armand, *Nat. Mater.* **2013** , 12, 452.

[11] F. Croce, G. B. Appetecchi, L. Persi and B. Scrosati,*Nature* . **1998** , 394, 456.

[12] H. Dang, B. Wang, Z. Chang, X. Wu, J. Feng, H. Zhou, W. Li and C. Sun, *ACS Sustain. Chem. Eng.* **2018** , 6, 13160-13167.

[13] X. Fang, W. Weng, J. Ren and H. Peng, *Adv. Mater.***2016** , 28, 491-496.

[14] J. Chang, Q. Huang, Y. Gao and Z. Zheng, *Adv. Mater.***2021** , 33, 2004419.

[15] K. S. Kumar, N. Choudhary, Y. Jung and J. Thomas, *ACS Energy Lett.* **2018** , 3, 482-495.

[16] L. Fan, K. Lin, J. Wang, R. Ma and B. Lu, *Adv. Mater.***2018** , 30, 1800804.

[17] V. Strauss, K. Marsh, M. D. Kowal, M. El-Kady and R. B. Kaner,*Adv. Mater.* **2018** , 30, 1704449.

[18] Y. Hu, D. Ye, B. Luo, H. Hu, X. Zhu, S. Wang, L. Li, S. Peng and L. Wang, *Adv. Mater.* **2018** , 30, 1703824.

[19. D. Sun, X. Zhu, B. Luo, Y. Zhang, Y. Tang, H. Wang and L. Wang,*Adv. Energy Mater* . **2018** , 8, 1801197.

[20] W. Zhao, M. Ding, L. Guo and H. Y. Yang, *Small* .**2019** , 15, 1805505.

[21] Y. Zhou, K. Maleski, B. Anasori, J. O. Thostenson, Y. Pang, Y. Feng, K. Zeng, C. B. Parker, S. Zauscher, Y. Gogotsi, J. T. Glass and C. Cao, *ACS Nano* . **2020** , 14, 3576-3586.

[22] P. Wang, Z. Chen, H. Wang, Z. Ji, Y. Feng, J. Wang, J. Liu, M. Hu, J. Fei, W. Gan and Y. Huang, *Energy Storage Mater* .**2020** , 25, 426-435.

[23] J. Orangi, F. Hamade, V. A. Davis and M. Beidaghi, *ACS Nano* , **2020** , 14, 640-650.

[24] W. Chen, X. Zhang, L. Mi, C. Liu, J. Zhang, S. Cui, X. Feng, Y. Cao and C. Shen, *Adv. Mater.* **2019** , 31, 1806664.

[25] X. Wang, Y. Zhang, X. Zhang, Z. Huo, X. Li, M. Que, Z. Peng, H. Wang and C. Pan, *Adv. Mater.* **2018** , 30, 1706738.

[26] Q. Zhang, X.-W. Gao, Y. Shi, W.-B. Luo, Y. Li, Q.-F. Gu, H.-N. Fan, F. Li and H.-K. Liu, *Energy Storage Mater.* **2021** , 39, 54-59.

[27] H. Li, Z. Liu, G. Liang, Y. Huang, Y. Huang, M. Zhu, Z. Pei, Q. Xue, Z. Tang, Y. Wang, B. Li and C. Zhi, *ACS Nano* , **2018** , 12, 3140-3148.

[28] C. Zhang, M. P. Kremer, A. Seral-Ascaso, S.-H. Park, N. McEvoy, B. Anasori, Y. Gogotsi and V. Nicolosi, *Advanced Functional Materials* , **2018** , 28, 1705506.

[29] J. Zhang, X. Zang, H. Wen, T. Dong, J. Chai, Y. Li, B. Chen, J. Zhao, S. Dong, J. Ma, L. Yue, Z. Liu, X. Guo, G. Cui and L. Chen,*J. Mater. Chem. A.* **2017** , 5, 4940-4948.

[30] Z. Deng, H. Jiang, Y. Hu, Y. Liu, L. Zhang, H. Liu and C. Li,*Adv. Mater.* **2017** , 29, 1603020.

[31] Z. Liu, Z.-S. Wu, S. Yang, R. Dong, X. Feng and K. Müllen,*Adv. Mater.* **2016** , 28, 2217-2222.

[32] K. Fu, Y. Gong, J. Dai, A. Gong, X. Han, Y. Yao, C. Wang, Y. Wang, Y. Chen, C. Yan, Y. Li, E. D. Wachsman and L. Hu, *Proc. Natl. Acad. Sci.* **2016** , 113, 7094-7099.

[33] F. Meng, H. Zhong, D. Bao, J. Yan and X. Zhang, *J. Am. Chem. Soc.* **2016** , 138, 10226-10231.

[34] T. M. Schmidt, T. T. Larsen-Olsen, J. E. Carlé, D. Angmo and F. C. Krebs, *Adv. Energy Mater.* **2015** , 5, 1500569.

[35] W. J. Hyun, E. B. Secor, M. C. Hersam, C. D. Frisbie and L. F. Francis, *Adv. Mater.* **2015** , 27, 109-115.

[36] G. Wang, H. Wang, X. Lu, Y. Ling, M. Yu, T. Zhai, Y. Tong and Y. Li, *Adv. Mater.* **2014** , 26, 2676-2682.

[37] L. Viry, A. Levi, M. Totaro, A. Mondini, V. Mattoli, B. Mazzolai and L. Beccai, *Adv. Mater.* **2014** , 26, 2659-2664.

[38] J. Liu, M. Chen, L. Zhang, J. Jiang, J. Yan, Y. Huang, J. Lin, H. J. Fan and Z. X. Shen, *Nano Lett* . **2014** , 14, 7180-7187.

[39] M. Amjadi, A. Pichitpajongkit, S. Lee, S. Ryu and I. Park,*ACS Nano* , **2014** , 8, 5154-5163.

[40] V. T. Le, H. Kim, A. Ghosh, J. Kim, J. Chang, Q. A. Vu, D. T. Pham, J.-H. Lee, S.-W. Kim and Y. H. Lee, *ACS Nano* ,**2013** , 7, 5940-5947.

[41] Y. Xu, Z. Lin, X. Huang, Y. Wang, Y. Huang and X. Duan,*Adv. Mater.* **2013** , 25, 5779-5784.

[42] Y. Meng, Y. Zhao, C. Hu, H. Cheng, Y. Hu, Z. Zhang, G. Shi and L. Qu, *Adv. Mater.* **2013** , 25, 2326-2331.

[43] Y. He, W. Chen, X. Li, Z. Zhang, J. Fu, C. Zhao and E. Xie,*ACS Nano* , **2013** , 7, 174-182.

[44] N. Li, Z. Chen, W. Ren, F. Li and H.-M. Cheng, *Proc. Natl. Acad. Sci.* **2012** , 109, 17360-17365

[45] F.-R. Fan, L. Lin, G. Zhu, W. Wu, R. Zhang and Z. L. Wang,*Nano Lett* . **2012** , 12, 3109-3114.

[46] L. Yuan, X.-H. Lu, X. Xiao, T. Zhai, J. Dai, F. Zhang, B. Hu, X. Wang, L. Gong, J. Chen, C. Hu, Y. Tong, J. Zhou and Z. L. Wang,*ACS Nano* . **2012** , 6, 656-661.

[47] M. F. El-Kady, V. Strong, S. Dubin and R. B. Kaner,*Science* . **2012** , 335, 1326-1330.

[48] Y. J. Yun, W. G. Hong, W.-J. Kim, Y. Jun and B. H. Kim,*Adv. Mater.* **2013** , 25, 5701-5705.

[49] D. Wakuda and K. Suganuma, *Appl. Phys. Lett.***2011** , 98, 073304.

[50] S. Zhu, J.-H. So, R. Mays, S. Desai, W. R. Barnes, B. Pourdeyhimi and M. D. Dickey, *Adv. Funct. Mater.* **2013** , 23, 2308-2314.

[51] Z. Xu, H. Sun, X. Zhao and C. Gao, *Adv. Mater.***2013** , 25, 188-193.

[52] H. Cheng, C. Hu, Y. Zhao and L. Qu, *Npg Asia Mater* ,**2014** , 6, e113.

[53] K. Amin, Q. Meng, A. Ahmad, M. Cheng, M. Zhang, L. Mao, K. Lu and Z. Wei, *Adv. Mater.* **2018** , 30, 1703868.

[54] J. Ren, Y. Zhang, W. Bai, X. Chen, Z. Zhang, X. Fang, W. Weng, Y. Wang and H. Peng, *Angew. Chem.* **2014** , 126, 7998-8003.

[55] H. Lin, W. Weng, J. Ren, L. Qiu, Z. Zhang, P. Chen, X. Chen, J. Deng, Y. Wang and H. Peng, *Adv. Mater.* **2014** , 26, 1217-1222.

[56] C.-F. Sun, H. Zhu, E. B. Baker Iii, M. Okada, J. Wan, A. Ghemes, Y. Inoue, L. Hu and Y. Wang, *Nano Energy* . **2013** , 2, 987-994.

[57] W. Weng, Q. Sun, Y. Zhang, H. Lin, J. Ren, X. Lu, M. Wang and H. Peng, *Nano Lett.* **2014** , 14, 3432-3438.

[58] Y. Zhang, W. Bai, X. Cheng, J. Ren, W. Weng, P. Chen, X. Fang, Z. Zhang and H. Peng, *Angew. Chem. Int. Ed.* **2014** , 53, 14564-14568.

[59] Y. Zhang, W. Bai, J. Ren, W. Weng, H. Lin, Z. Zhang and H. Peng, *J. Mater. Chem. A* . **2014** , 2, 11054-11059.

[60] B. Fang, D. Chang, Z. Xu and C. Gao, *Adv. Mater.***2020** , 32, 1902664.

[61] Y. Zhou, C.-H. Wang, W. Lu and L. Dai, *Adv. Mater.***2020** , 32, 1902779.

[62] L. Wang, X. Fu, J. He, X. Shi, T. Chen, P. Chen, B. Wang and H. Peng, *Adv. Mater.* **2020** , 32, 1901971.

[63] D. Chen, K. Jiang, T. Huang and G. Shen, *Adv. Mater.***2020** , 32, 1901806.

[64] Z. Dong, C. Jiang, H. Cheng, Y. Zhao, G. Shi, L. Jiang and L. Qu, *Adv. Mater.* **2012** , 24, 1856-1861.

[65] H. Cheng, J. Liu, Y. Zhao, C. Hu, Z. Zhang, N. Chen, L. Jiang and L. Qu, *Angew. Chem. Int. Ed.* **2013** , 52, 10482-10486.

[66] H. Cheng, Y. Hu, F. Zhao, Z. Dong, Y. Wang, N. Chen, Z. Zhang and L. Qu, *Adv. Mater.* **2014** , 26, 2909-2913.

[67] Z. Yang, H. Sun, T. Chen, L. Qiu, Y. Luo and H. Peng,*Angew. Chem. Int. Ed.* **2013** , 52, 7545-7548.

[68] Z. Xu, Z. Liu, H. Sun and C. Gao, *Adv. Mater.***2013** , 25, 3249-3253.

[69] J. Yu, W. Lu, J. P. Smith, K. S. Booksh, L. Meng, Y. Huang, Q. Li, J.-H. Byun, Y. Oh, Y. Yan and T.-W. Chou, *Adv. Energy Mater* .**2017** , 7, 1600976.

[70] Z. Wen, M.-H. Yeh, H. Guo, J. Wang, Y. Zi, W. Xu, J. Deng, L. Zhu, X. Wang, C. Hu, L. Zhu, X. Sun and Z. L. Wang, *Sci. Adv* .**2016** , 2, e1600097.

[71] J. Bae, M. K. Song, Y. J. Park, J. M. Kim, M. Liu and Z. L. Wang, *Angew. Chem. Int. Ed.* , **2011** , 50, 1683-1687.

[72] X. Zheng, L. Yao, Y. Qiu, S. Wang and K. Zhang, *ACS Applied Energy Materials* , **2019** , 2, 4335-4344.

[73] S. Wang, N. Liu, J. Su, L. Li, F. Long, Z. Zou, X. Jiang and Y. Gao, *ACS Nano* , **2017** , 11, 2066-2074.

[74] K. Keum, G. Lee, H. Lee, J. Yun, H. Park, S. Y. Hong, C. Song, J. W. Kim and J. S. Ha, *ACS Applied Materials & Interfaces* ,**2018** , 10, 26248-26257.

[75] X. Dong, Z. Guo, Y. Song, M. Hou, J. Wang, Y. Wang and Y. Xia,*Adv. Funct. Mater.* **2014** , 24, 3405-3412.

[76] X. Pu, L. Li, M. Liu, C. Jiang, C. Du, Z. Zhao, W. Hu and Z. L. Wang, *Adv. Mater.* , **2016** , 28, 98-105.

[77] Y. Huang, W. S. Ip, Y. Y. Lau, J. Sun, J. Zeng, N. S. S. Yeung, W. S. Ng, H. Li, Z. Pei, Q. Xue, Y. Wang, J. Yu, H. Hu and C. Zhi,*ACS Nano* , **2017** , 11, 8953-8961.

[78] W. G. Chong, J.-Q. Huang, Z.-L. Xu, X. Qin, X. Wang and J.-K. Kim, *Adv. Funct. Mater.* **2017** , 27, 1604815.

[79] Y. H. Kwon, S.-W. Woo, H.-R. Jung, H. K. Yu, K. Kim, B. H. Oh, S. Ahn, S.-Y. Lee, S.-W. Song, J. Cho, H.-C. Shin and J. Y. Kim,*Adv. Mater.* **2012** , 24, 5192-5197.

[80] Y.-h. Zhu, S. Yuan, D. Bao, Y.-b. Yin, H.-X. Zhong, X.-b. Zhang, J.-m. Yan and Q. Jiang, *Adv. Mater.* **2017** , 29, 1603719.

[81] Q. Chen, S. Sun, T. Zhai, M. Yang, X. Zhao and H. Xia,*Adv. Energy. Mater.* **2018** , 8, 1800054.

[82] H. Sun, X. You, J. Deng, X. Chen, Z. Yang, J. Ren and H. Peng,*Adv. Mater.* , **2014** , 26, 2868-2873.

[83] Z. Zhang, X. Chen, P. Chen, G. Guan, L. Qiu, H. Lin, Z. Yang, W. Bai, Y. Luo and H. Peng, *Adv. Mater.* **2014** , 26, 466-470.

[84] J. Wang, X. Li, Y. Zi, S. Wang, Z. Li, L. Zheng, F. Yi, S. Li and Z. L. Wang, *Adv. Mater.* **2015** , 27, 4830-4836.

[85] K. Dong, Y.-C. Wang, J. Deng, Y. Dai, S. L. Zhang, H. Zou, B. Gu, B. Sun and Z. L. Wang, *ACS Nano* , **2017** , 11, 9490-9499.

[86] F. Liu, S. Song, D. Xue and H. Zhang, *Adv. Mater.***2012** , 24, 1089-1094.

[87] H. Gwon, H.-S. Kim, K. U. Lee, D.-H. Seo, Y. C. Park, Y.-S. Lee, B. T. Ahn and K. Kang, *Energy Environ. Sci.* **2011** , 4, 1277-1283.

[88] Y. Meng, K. Wang, Y. Zhang and Z. Wei, *Adv. Mater.***2013** , 25, 6985-6990.

[89] V. L. Pushparaj, M. M. Shaijumon, A. Kumar, S. Murugesan, L. Ci, R. Vajtai, R. J. Linhardt, O. Nalamasu and P. M. Ajayan, *Proc. Natl. Acad. Sci.* **2007** , 104, 13574-13577.

[90] L. Hu, H. Wu, F. La Mantia, Y. Yang and Y. Cui, *ACS Nano* , **2010** , 4, 5843-5848.

[91] X. Xiao, X. Peng, H. Jin, T. Li, C. Zhang, B. Gao, B. Hu, K. Huo and J. Zhou, *Adv. Mater.* **2013** , 25, 5091-5097.

[92] H. Wang, L.-F. Cui, Y. Yang, H. Sanchez Casalongue, J. T. Robinson, Y. Liang, Y. Cui and H. Dai, *J. Am. Chem. Soc.* ,**2010** , 132, 13978-13980.

[93] D. Wang, D. Choi, J. Li, Z. Yang, Z. Nie, R. Kou, D. Hu, C. Wang, L. V. Saraf, J. Zhang, I. A. Aksay and J. Liu, *ACS Nano* .**2009** , 3, 907-914.

[94] S.-M. Paek, E. Yoo and I. Honma, *Nano Lett.***2009** , 9, 72-75.

[95] J. Wu, X. Gao, H. Yu, T. Ding, Y. Yan, B. Yao, X. Yao, D. Chen, M. Liu and L. Huang, *Adv. Funct. Mater.* **2016** , 26, 6114-6120.

[96] W. H. Shin, H. M. Jeong, B. G. Kim, J. K. Kang and J. W. Choi,*Nano Lett.* , **2012** , 12, 2283-2288.

[97] A. L. M. Reddy, A. Srivastava, S. R. Gowda, H. Gullapalli, M. Dubey and P. M. Ajayan, *ACS Nano* . **2010** , 4, 6337-6342.

[98] A. S. Aricò, P. Bruce, B. Scrosati, J.-M. Tarascon and W. van Schalkwijk, *Nat. Mater* . **2005** , 4, 366.

[99] B. Liu, J. Zhang, X. Wang, G. Chen, D. Chen, C. Zhou and G. Shen, *Nano Lett.* **2012** , 12, 3005-3011.

[100] X. Jia, Z. Chen, A. Suwarnasarn, L. Rice, X. Wang, H. Sohn, Q. Zhang, B. M. Wu, F. Wei and Y. Lu, *Energy Environ. Sci.***2012** , 5, 6845-6849.

[101] L. David, R. Bhandavat and G. Singh, *ACS Nano* .**2014** , 8, 1759-1770.

[102] Y. Liu, Y. Fang, Z. Zhao, C. Yuan and X. W. Lou, *Adv. Energy. Mater.* **2019** , 9, 1803052.

[103] Y.-H. Zhu, X. Yang, D. Bao, X.-F. Bie, T. Sun, S. Wang, Y.-S. Jiang, X.-B. Zhang, J.-M. Yan and Q. Jiang, *Joule* . **2018** , 2, 736-746.

[104] J.-Y. Choi, D. J. Lee, Y. M. Lee, Y.-G. Lee, K. M. Kim, J.-K. Park and K. Y. Cho, *Adv. Funct. Mater.* **2013** , 23, 2108-2114.

[105] X. Zhao, C. M. Hayner, M. C. Kung and H. H. Kung, *Adv. Energy Mater* . **2011** , 1, 1079-1084.

[106] J. K. Lee, K. B. Smith, C. M. Hayner and H. H. Kung,*Chem. Commun.* **2010** , 46, 2025-2027.

[107] H. Zhang, S. Jing, Y. Hu, H. Jiang and C. Li, *J Power Sources* . **2016** , 307, 214-219.

[108] Y. Zeng, Z. Lin, Y. Meng, Y. Wang, M. Yu, X. Lu and Y. Tong,*Adv. Mater.* **2016** , 28, 9188-9195.

[109] M. Gong, Y. Li, H. Zhang, B. Zhang, W. Zhou, J. Feng, H. Wang, Y. Liang, Z. Fan, J. Liu and H. Dai, *Energy Environ. Sci.***2014** , 7, 2025-2032.

[110] U. Köhler, C. Antonius and P. Bäuerlein, *J Power Sources* . **2004** , 127, 45-52.

[111] H. Pan, Y. Shao, P. Yan, Y. Cheng, K. S. Han, Z. Nie, C. Wang, J. Yang, X. Li, P. Bhattacharya, K. T. Mueller and J. Liu, *Nature Energy* . **2016** , 1, 16039.

[112] F. Y. Cheng, J. Chen, X. L. Gou and P. W. Shen, *Adv. Mater.* **2005** , 17, 2753-2756.

[113] B. J. Hertzberg, A. Huang, A. Hsieh, M. Chamoun, G. Davies, J. K. Seo, Z. Zhong, M. Croft, C. Erdonmez, Y. S. Meng and D. Steingart,*Chem. Mater.* **2016** , 28, 4536-4545.

[114] C. Xu, B. Li, H. Du and F. Kang, *Angew. Chem.***2012** , 124, 957-959.

[115] C.-C. Yang and S.-J. Lin, *J Power Sources* .**2002** , 112, 174-183.

[116] M. Pasta, C. D. Wessells, R. A. Huggins and Y. Cui, *Nat. Commun* . **2012** , 3, 1149.

[117] Y. Lu, J. B. Goodenough and Y. Kim, *J. Am. Chem. Soc.***2011** , 133, 5756-5759.

[118] C. Guan, W. Zhao, Y. Hu, Q. Ke, X. Li, H. Zhang and J. Wang,*Adv. Energy Mater* . **2016** , 6, 1601034.

[119] H. Wang, Y. Liang, M. Gong, Y. Li, W. Chang, T. Mefford, J. Zhou, J. Wang, T. Regier, F. Wei and H. Dai, *Nat. Commun* .**2012** , 3, 917.

[120] C. Chakkaravarthy, P. Periasamy, S. Jegannathan and K. I. Vasu, *J Power Sources.* **1991** , 35, 21-35.

[121] J. Liu, C. Guan, C. Zhou, Z. Fan, Q. Ke, G. Zhang, C. Liu and J. Wang, *Adv. Mater.* **2016** , 28, 8732-8739.

[122] C. Li, Q. Zhang, J. Sun, T. Li, S. E, Z. Zhu, B. He, Z. Zhou, Q. Li and Y. Yao, *ACS Energy Letters* . **2018** , 3, 2761-2768.

[123] G. G. Amatucci, F. Badway, A. Du Pasquier and T. Zheng,*J. Electrochem. Soc.* **2001** , 148, A930-A939.

[124] R. Satish, V. Aravindan, W. C. Ling and S. Madhavi, *J Power Sources* . **2015** , 281, 310-317.

[125] E. Lim, C. Jo, H. Kim, M.-H. Kim, Y. Mun, J. Chun, Y. Ye, J. Hwang, K.-S. Ha, K. C. Roh, K. Kang, S. Yoon and J. Lee, *ACS Nano* . **2015** , 9, 7497-7505.

[126] Y. Zhang, X. Jing, Q. Wang, J. Zheng, H. Jiang and C. Meng,*Dalton Trans.* **2017** , 46, 15048-15058.

[127] X. Hu, Z. Deng, J. Suo and Z. Pan, *J Power Sources* .**2009** , 187, 635-639.

[128] J. Jiang, G. Tan, S. Peng, D. Qian, J. Liu, D. Luo and Y. Liu,*Electrochim. Acta* . **2013** , 107, 59-65.

[129] R. Li, Y. Wang, C. Zhou, C. Wang, X. Ba, Y. Li, X. Huang and J. Liu, *Adv. Funct. Mater.* **2015** , 25, 5384-5394.

[130] H. Li, L. Peng, Y. Zhu, X. Zhang and G. Yu, *Nano Lett.***2016** , 16, 5938-5943.

[131] W. Wang, M. Tang, Z. Zheng and S. Chen, *Adv. Energy Mater* . **2019** , 9, 1803628.

[132] G. Zhou, S. Pei, L. Li, D.-W. Wang, S. Wang, K. Huang, L.-C. Yin, F. Li and H.-M. Cheng, *Adv. Mater.* **2014** , 26, 625-631.

[133] L. Ma, W. Zhang, L. Wang, Y. Hu, G. Zhu, Y. Wang, R. Chen, T. Chen, Z. Tie, J. Liu and Z. Jin, *ACS Nano* . **2018** , 12, 4868-4876.

[134] M. Yao, R. Wang, Z. Zhao, Y. Liu, Z. Niu and J. Chen,*ACS Nano* . **2018** , 12, 12503-12511.

[135] X. Chen, B. Liu, C. Zhong, Z. Liu, J. Liu, L. Ma, Y. Deng, X. Han, T. Wu, W. Hu and J. Lu, *Adv. Energy Mater* . **2017** , 7, 1700779.

[136] Q.-C. Liu, L. Li, J.-J. Xu, Z.-W. Chang, D. Xu, Y.-B. Yin, X.-Y. Yang, T. Liu, Y.-S. Jiang, J.-M. Yan and X.-B. Zhang, *Adv. Mater.* **2015** , 27, 8095-8101.

[137] M. Koo, K.-I. Park, S. H. Lee, M. Suh, D. Y. Jeon, J. W. Choi, K. Kang and K. J. Lee, *Nano Lett.* **2012** , 12, 4810-4816.

[138] M. C. McAlpine, H. Ahmad, D. Wang and J. R. Heath, *Nat. Mater* . **2007** , 6, 379.

[139] Z. Weng, Y. Su, D.-W. Wang, F. Li, J. Du and H.-M. Cheng,*Adv. Energy Mater* . **2011** , 1, 917-922.

[140] Z. S. Wu, K. Parvez, X. Feng and K. Müllen, *Nat. Commun* . **2013** , 4, 2487.

[141] J.-X. Feng, S.-H. Ye, A.-L. Wang, X.-F. Lu, Y.-X. Tong and G.-R. Li, *Adv. Funct. Mater.* **2014** , 24, 7093-7101.

[142] Y. Chen, K. Cai, C. Liu, H. Song and X. Yang, *Adv. Energy Mater* . **2017** , 7, 1701247.

[143] X. Xue, Y. Fu, Q. Wang, L. Xing and Y. Zhang, *Adv. Funct. Mater.* **2016** , 26, 3128-3138.

[144] X. Ren, H. Fan, Y. Zhao and Z. Liu, *ACS Appl. Mater. Interfaces* . **2016** , 8, 26190-26197.

[145] A. Sultana, M. M. Alam, S. Garain, T. K. Sinha, T. R. Middya and D. Mandal, *ACS Appl. Mater. Interfaces* . **2015** , 7, 19091-19097.

[146] Q. Zheng, H. Zhang, H. Mi, Z. Cai, Z. Ma and S. Gong,*Nano Energy* . **2016** , 26, 504-512.

[147] J. Lee, J. Wu, M. Shi, J. Yoon, S.-I. Park, M. Li, Z. Liu, Y. Huang and J. A. Rogers, *Adv. Mater.* **2011** , 23, 986-991.

[148] A. Koh, D. Kang, Y. Xue, S. Lee, R. M. Pielak, J. Kim, T. Hwang, S. Min, A. Banks, P. Bastien, M. C. Manco, L. Wang, K. R. Ammann, K.-I. Jang, P. Won, S. Han, R. Ghaffari, U. Paik, M. J. Slepian, G. Balooch, Y. Huang and J. A. Rogers, *Science Translational Medicine* . **2016** , 8, 366ra165-366ra165.

[149] J. Kim, M. Lee, H. J. Shim, R. Ghaffari, H. R. Cho, D. Son, Y. H. Jung, M. Soh, C. Choi, S. Jung, K. Chu, D. Jeon, S.-T. Lee, J. H. Kim, S. H. Choi, T. Hyeon and D.-H. Kim, *Nat. Commun* .**2014** , 5, 5747.

[150] S. C. B. Mannsfeld, B. C. K. Tee, R. M. Stoltenberg, C. V. H. H. Chen, S. Barman, B. V. O. Muir, A. N. Sokolov, C. Reese and Z. Bao,*Nat. Mater* . **2010** , 9, 859.

[151] M. Zirkl, A. Haase, A. Fian, H. Schön, C. Sommer, G. Jakopic, G. Leising, B. Stadlober, I. Graz, N. Gaar, R. Schwödiauer, S. Bauer-Gogonea and S. Bauer, *Adv. Mater.* **2007** , 19, 2241-2245.

[152] M. Sibinski, M. Jakubowska and M. Sloma, *Sensors* .**2010** , 10, 7934.

[153] D.-H. Kim, N. Lu, R. Ma, Y.-S. Kim, R.-H. Kim, S. Wang, J. Wu, S. M. Won, H. Tao, A. Islam, K. J. Yu, T.-i. Kim, R. Chowdhury, M. Ying, L. Xu, M. Li, H.-J. Chung, H. Keum, M. McCormick, P. Liu, Y.-W. Zhang, F. G. Omenetto, Y. Huang, T. Coleman and J. A. Rogers, *Science* .**2011** , 333, 838-843.

[154] Z. Chen, W. Ren, L. Gao, B. Liu, S. Pei and H.-M. Cheng,*Nat. Mater* . **2011** , 10, 424-428.

[155] Z. Chen, C. Xu, C. Ma, W. Ren and H.-M. Cheng, *Adv. Mater.* **2013** , 25, 1296-1300.

[156] B. Chen, W. Tang, T. Jiang, L. Zhu, X. Chen, C. He, L. Xu, H. Guo, P. Lin, D. Li, J. Shao and Z. L. Wang, *Nano Energy* .**2018** , 45, 380-389.

[157] C. Wu, J. H. Park, B. Koo, X. Chen, Z. L. Wang and T. W. Kim,*ACS Nano* . **2018** , 12, 9947-9957.

[158] Z. Qi, J. Ye, W. Chen, J. Biener, E. B. Duoss, C. M. Spadaccini, M. A. Worsley and C. Zhu, *Adv. Mater. Tech.***2018** , 3, 1800053.

[159] G. Chen, R. Rastak, Y. Wang, H. Yan, V. Feig, Y. Liu, Y. Jiang, S. Chen, F. Lian, F. Molina-Lopez, L. Jin, K. Cui, J. W. Chung, E. Pop, C. Linder and Z. Bao, *Matter* . **2019** , 1, 205–218.

[160] Y. Xu, Z. Lin, X. Huang, Y. Liu, Y. Huang and X. Duan,*ACS Nano* . **2013** , 7, 4042-4049.

[161] Y. Shi, L. Pan, B. Liu, Y. Wang, Y. Cui, Z. Bao and G. Yu,*J. Mater. Chem. A* . **2014** , 2, 6086-6091.

[162] Y. Zhao, J. Liu, Y. Hu, H. Cheng, C. Hu, C. Jiang, L. Jiang, A. Cao and L. Qu, *Adv. Mater.* **2013** , 25, 591-595.

[163] X. Zhang, Z. Lin, B. Chen, W. Zhang, S. Sharma, W. Gu and Y. Deng, *J Power Sources* . **2014** , 246, 283-289.

[164] Z. Tang, L. Gao, Y. Wu, T. Su, Q. Wu, X. Liu, W. Li and Q. Wang, *J. Mater. Chem. B* . **2013** , 1, 5393-5397.

[165] L. Han, X. Lu, M. Wang, D. Gan, W. Deng, K. Wang, L. Fang, K. Liu, C. W. Chan, Y. Tang, L.-T. Weng and H. Yuan, *Small* .**2017** , 13, 1601916.

[166] G. A. Salvatore, N. Münzenrieder, T. Kinkeldei, L. Petti, C. Zysset, I. Strebel, L. Büthe and G. Tröster, *Nat. Commun* .**2014** , 5, 2982.

[167] S. Harada, K. Kanao, Y. Yamamoto, T. Arie, S. Akita and K. Takei, *ACS Nano* . **2014** , 8, 12851-12857.

[168] X. Jin, L. Song, H. Yang, C. Dai, Y. Xiao, X. Zhang, Y. Han, C. Bai, B. Lu, Q. Liu, Y. Zhao, J. Zhang, Z. Zhang and L. Qu,*Energ. Environ. Sci.* **2021** , 14, 3075-3085

[169] Z. L. Wang and J. Song, *Science* . **2006** , 312, 242-246.

[170] K.-I. Park, J. H. Son, G.-T. Hwang, C. K. Jeong, J. Ryu, M. Koo, I. Choi, S. H. Lee, M. Byun, Z. L. Wang and K. J. Lee, *Adv. Mater.* **2014** , 26, 2514-2520.

[171] L. Lin, S. Wang, Y. Xie, Q. Jing, S. Niu, Y. Hu and Z. L. Wang, *Nano Lett.* **2013** , 13, 2916-2923.

[172] Y. Yang, W. Guo, K. C. Pradel, G. Zhu, Y. Zhou, Y. Zhang, Y. Hu, L. Lin and Z. L. Wang, *Nano Lett.* **2012** , 12, 2833-2838.

[173] W. Zeng, L. Shu, Q. Li, S. Chen, F. Wang and X.-M. Tao,*Adv. Mater.* **2014** , 26, 5310-5336.

[174] Y. Qi and M. C. McAlpine, *Energy Environ. Sci.***2010** , 3, 1275-1285.

[175] Z. L. Wang, *Adv. Funct. Mater.* **2008** , 18, 3553-3567.

[176] X. Wang, J. Song, J. Liu and Z. L. Wang, *Science* .**2007** , 316, 102-105.

[177] P. X. Gao, J. Song, J. Liu and Z. L. Wang, *Adv. Mater.***2007** , 19, 67-72.

[178] J. M. Donelan, Q. Li, V. Naing, J. A. Hoffer, D. J. Weber and A. D. Kuo, *Science* . **2008** , 319, 807-810.

[179] C. A. Angell, C. Liu and E. Sanchez, *Nature* .**1993** , 362, 137.

[180] Y. Huang, M. Zhong, Y. Huang, M. Zhu, Z. Pei, Z. Wang, Q. Xue, X. Xie and C. Zhi, *Nat. Commun* . **2015** , 6, 10310.

[181] Q. Ma, H. Zhang, C. Zhou, L. Zheng, P. Cheng, J. Nie, W. Feng, Y.-S. Hu, H. Li, X. Huang, L. Chen, M. Armand and Z. Zhou, *Angew. Chem. Int. Ed.* **2016** , 55, 2521-2525.

[182] J. Wan, J. Xie, X. Kong, Z. Liu, K. Liu, F. Shi, A. Pei, H. Chen, W. Chen, J. Chen, X. Zhang, L. Zong, J. Wang, L.-Q. Chen, J. Qin and Y. Cui, *Nat. Nanotech* . **2019** , 14, 705-711.

[183] L. Chen, Y. Li, S.-P. Li, L.-Z. Fan, C.-W. Nan and J. B. Goodenough, *Nano Energy* . **2018** , 46, 176-184.

[184] S. Feng, D. Shi, F. Liu, L. Zheng, J. Nie, W. Feng, X. Huang, M. Armand and Z. Zhou, *Electrochim. Acta* . **2013** , 93, 254-263.

[185] H.-J. Ha, E.-H. Kil, Y. H. Kwon, J. Y. Kim, C. K. Lee and S.-Y. Lee, *Energ. Environ. Sci.* **2012** , 5, 6491-6499.

[186] D. Wei, S. Haque, P. Andrew, J. Kivioja, T. RyhÃ¤nen, A. Pesquera, A. Centeno, B. Alonso, A. Chuvilin and A. Zurutuza, *J. Mater. Chem. A.* **2013** , 1, 3177-3181.

[187] R. Rohan, K. Pareek, W. Cai, Y. Zhang, G. Xu, Z. Chen, Z. Gao, Z. Dan and H. Cheng, *J. Mater. Chem. A* . **2015** , 3, 5132-5139.

[188] S. Saricilar, D. Antiohos, K. Shu, P. G. Whitten, K. Wagner, C. Wang and G. G. Wallace, *Electrochem. Commun.* **2013** , 32, 47-50.

[189] J.-i. Kadokawa, N. Egashira and K. Yamamoto,*Biomacromolecules* . **2018** , 19, 3013-3019.

[190] H. Yu, J. Wu, L. Fan, Y. Lin, K. Xu, Z. Tang, C. Cheng, S. Tang, J. Lin, M. Huang and Z. Lan, *J Power Sources* .**2012** , 198, 402-407.

[191] C. Zhao, C. Wang, Z. Yue, K. Shu and G. G. Wallace, *ACS Appl. Mater. Interfaces* . **2013** , 5, 9008-9014.

[192] E. J. Cheng, T. Kimura, M. Shoji, H. Ueda, H. Munakata and K. Kanamura, *ACS Applied Materials & Interfaces* , **2020** , 12, 10382-10388.

[193] T. Jiang, P. He, G. Wang, Y. Shen, C.-W. Nan and L.-Z. Fan,*Adv. Energy Mater.* **2020** , 10, 1903376.

[194] M. M. E. Jacob, E. Hackett and E. P. Giannelis, *J. Mater. Chem.* **2003** , 13, 1-5.

[195] W. Liu, N. Liu, J. Sun, P.-C. Hsu, Y. Li, H.-W. Lee and Y. Cui, *Nano Lett.* **2015** , 15, 2740-2745.

[196] J. Zheng, M. Tang and Y.-Y. Hu, *Angew. Chem. Int. Ed* .**2016** , 55, 12538-12542.

[197] W. Zhou, S. Wang, Y. Li, S. Xin, A. Manthiram and J. B. Goodenough, *J. Am. Chem. Soc.* **2016** , 138, 9385-9388.

[198] Z. Wang, R. Pan, R. Sun, K. Edström, M. Strømme and L. Nyholm,*ACS Appl. Energy Mater.* **2018** , 1, 4341-4350.

[199] J. Liu, T. Qian, M. Wang, J. Zhou, N. Xu and C. Yan,*Nano Lett.* **2018** , 18, 4598-4605.

[200] D. Zhang, X. Xu, X. Huang, Z. Shi, Z. Wang, Z. Liu, R. Hu, J. Liu and M. Zhu, *J. Mater. Chem. A* . **2020** , 8, 18043-18054.

[201] H. Huo, Y. Chen, J. Luo, X. Yang, X. Guo and X. Sun,*Adv. Energy Mater.* **2019** , 9, 1804004.